Chapter 18

Black Holes

A spectacular consequences of GR is the prediction that

- gravitational fields can become so strong that they can effectively trap even light,
- because space becomes so curved that there are no paths for light from an interior to exterior region.

Such objects are called *black holes*.

We shall discuss 2 solutions to GR that can lead to black holes:

- The *Schwarzschild solution*, which can be used to describe spherical black holes with no charge or angular momentum
- The *Kerr solution*, which can be used to describe rotating, uncharged black holes.

We shall also consider how gravity is altered if *quantum mechanics* comes into play, and consider *observational evidence* for black holes.

18.1 The Schwarzschild Solution

One of the simplest solutions corresponds to a metric that describes the gravitational field exterior to a static, spherical, uncharged mass without angular momentum and isolated from all other mass (Schwarzschild, 1916).

The Schwarzschild solution is

- A solution to the vacuum Einstein equations $G_{\mu\nu} = R_{\mu\nu} = 0$.
- Thus valid only in the absence of matter and non-gravitational fields ($T_{\mu\nu} = 0$).
- Spherically symmetric.

Thus, the Schwarzschild solution is valid outside spherical mass distributions, but the interior of a star will be described by a different metric that must be matched at the surface to the Schwarzschild one.

18.1.1 The Form of the Metric

Work in spherical coordinates (r, θ, φ) and seek a time-independent solution assuming

- The angular part of the metric will be unchanged from its form in flat space because of the spherical symmetry.
- The parts of the metric describing t and r will be modified by functions that depend on the radial coordinate r.

Therefore, let us write the 4-D line element as

$$ds^2 = \underbrace{-B(r)dt^2 + A(r)dr^2}_{\text{Modified from flat space}} \quad \underbrace{+r^2 d\theta^2 + r^2 \sin^2\theta d\varphi^2}_{\text{Same as flat space}},$$

where $A(r)$ and $B(r)$ are unknown functions that may depend on r but not time. They may be determined by

1. Requiring that this metric be consistent with the Einstein field equations for $T_{\mu\nu} = 0$.
2. Imposing physical boundary conditions.

Boundary conditions: Far from the star gravity becomes weak so

$$\lim_{r\to\infty} A(r) = \lim_{r\to\infty} B(r) = 1.$$

Substitute the metric form in vacuum Einstein and impose these boundary conditions (Exercise):

1. With the assumed form of the metric,

$$g_{\mu\nu} = \begin{pmatrix} -B(r) & 0 & 0 & 0 \\ 0 & A(r) & 0 & 0 \\ 0 & 0 & r^2 & 0 \\ 0 & 0 & 0 & r^2\sin^2\theta \end{pmatrix}.$$

   compute the non-vanishing connection coefficients $\Gamma^{\lambda}_{\mu\nu}$.

$$\Gamma^{\sigma}_{\lambda\mu} = \tfrac{1}{2} g^{\nu\sigma}\left(\frac{\partial g_{\mu\nu}}{\partial x^{\lambda}} + \frac{\partial g_{\lambda\nu}}{\partial x^{\mu}} - \frac{\partial g_{\mu\lambda}}{\partial x^{\nu}}\right)$$

2. Use the connection coefficients to construct the Ricci tensor $R_{\mu\nu}$.

$$R_{\mu\nu} = \Gamma^{\lambda}_{\mu\nu,\lambda} - \Gamma^{\lambda}_{\mu\lambda,\nu} + \Gamma^{\lambda}_{\mu\nu}\Gamma^{\sigma}_{\lambda\sigma} - \Gamma^{\sigma}_{\mu\lambda}\Gamma^{\lambda}_{\nu\sigma},$$

   (Only need $R_{\mu\nu}$, not full $G_{\mu\nu}$, since we will solve *vacuum Einstein equations.*

3. Solve the coupled set of equations

$$R_{\mu\nu} = 0$$

subject to the boundary conditions

$$\lim_{r\to\infty} A(r) = \lim_{r\to\infty} B(r) = 1.$$

The solution requires some manipulation but is remarkably simple:

$$B(r) = 1 - \frac{2M}{r} \qquad A(r) = B(r)^{-1},$$

where M is the single parameter. The line element is then

$$ds^2 = -\left(1 - \frac{2M}{r}\right) dt^2 + \left(1 - \frac{2M}{r}\right)^{-1} dr^2 + r^2 d\theta^2 + r^2 \sin^2\theta\, d\varphi^2,$$

where $d\tau^2 = -ds^2$. The corresponding metric tensor is

$$g_{\mu\nu} = \begin{pmatrix} -\left(1 - \frac{2M}{r}\right) & 0 & 0 & 0 \\ 0 & \left(1 - \frac{2M}{r}\right)^{-1} & 0 & 0 \\ 0 & 0 & r^2 & 0 \\ 0 & 0 & 0 & r^2 \sin^2\theta \end{pmatrix}.$$

which is diagonal but *not constant.*

By comparing

$$\underbrace{g_{00} = -\left(1 - \frac{2GM}{rc^2}\right)}_{\text{Weak gravity (earlier)}} \quad \longleftrightarrow \quad \underbrace{g_{00} = -\left(1 - \frac{2GM}{rc^2}\right)}_{\text{Schwarzschild } (G \,\&\, c \text{ restored})}$$

we see that the parameter M (mathematically the single free parameter of the solution) may be identified with the total mass that is the source of the gravitational curvature. It has 3 contributions:

- Rest mass
- Contributions from mass–energy densities and pressure
- Energy from spacetime curvature

From the structure of the metric

$$ds^2 = -B(r)dt^2 + A(r)dr^2 + r^2 d\theta^2 + r^2 \sin^2\theta d\varphi^2,$$

- θ and φ have similar interpretations as for flat space.
- r generally *cannot be interpreted as a radius* because $A(r) \neq 1$.
- The coordinate time t generally *cannot be interpreted as a clock time* because $B(r) \neq 1$.

The quantity

$$r_S \equiv 2M$$

is called the *Schwarzschild radius.* It plays a central role in the description of the Schwarzschild spacetime.

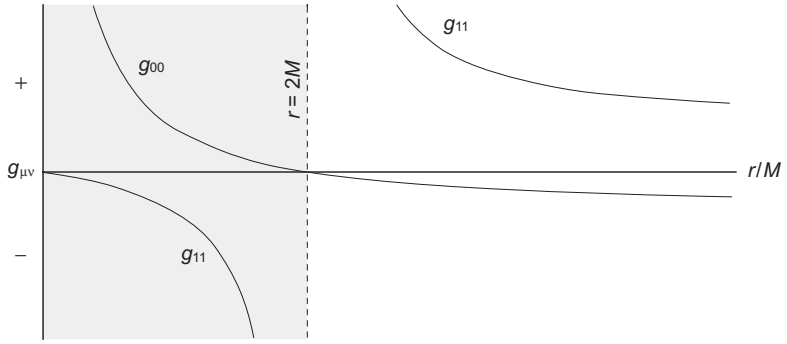

Figure 18.1: The components g_{00} and g_{11} in the Schwarzschild metric.

The line element (metric)

$$ds^2 = -\left(1 - \frac{2M}{r}\right) dt^2 + \left(1 - \frac{2M}{r}\right)^{-1} dr^2 + r^2 d\theta^2 + r^2 \sin^2\theta d\varphi^2$$

appears to contain two singularities

1. A singularity at $r = 0$ (an *essential singularity*).
2. A singularity at $r = r_S = 2M$ (a *coordinate singularity*).

Coordinate Singularity: Place where a chosen set of coordinates does not describe the geometry properly.

Example: At North Pole the azimuthal angle φ takes a continuum of values 0–2π, so all those values correspond to a single point. But this has *no physical significance.*

Coordinate singularities not essential and can be removed by a *different choice of coordinate system.*

18.1.2 Measuring Distance and Time

What is the physical meaning of the coordinates (t, r, θ, φ)?

- We may assign a practical definition to the radial coordinate r by
  1. Enclosing the origin of our Schwarzschild spacetime in a series of concentric spheres,
  2. Measuring for each sphere a surface area (conceptually by laying measuring rods end to end),
  3. Assigning a radial coordinate r to that sphere using Area $= 4\pi r^2$.
- Then we can use distances and trigonometry to define the angular coordinate variables θ and φ.
- Finally we can define coordinate time t in terms of clocks attached to the concentric spheres.

> For Newtonian theory with its implicit assumption that events occur on a passive background of euclidean space and constantly flowing time, that's the whole story.

But in curved Schwarzschild spacetime

- The coordinates (t, r, θ, φ) provide a global reference frame for an observer making measurements an infinite distance from the gravitational source of the Schwarzschild spacetime.
- However, physical quantities measured by arbitrary observers are not specified directly by these coordinates but rather must be computed from the metric.

Proper and Coordinate Distances

Consider distance measured in the radial direction. Set $dt = d\theta = d\varphi = 0$ in the line element to obtain an interval of radial distance

$$ds^2 = -\left(1 - \frac{2M}{r}\right)\underbrace{dt^2}_{=0} + \left(1 - \frac{2M}{r}\right)^{-1} dr^2 + r^2\underbrace{d\theta^2}_{=0} + r^2 \sin^2\theta \underbrace{d\varphi^2}_{=0}$$

$$\longrightarrow \quad ds^2 = \left(1 - \frac{2M}{r}\right)^{-1} dr^2 \quad \longrightarrow \quad ds = \frac{dr}{\sqrt{1 - \frac{2GM}{rc^2}}},$$

- In this expression we term ds the *proper distance* and dr the *coordinate distance.*
- The physical interval in the radial direction measured by a local observer is given by the proper distance ds, *not by* dr.
- GM/rc^2 is a measure of the strength of gravity so the proper distance and coordinate distance are equivalent only if gravity is negligibly weak, either because
  1. The source M is small, or
  2. we are a very large coordinate distance r from the source.

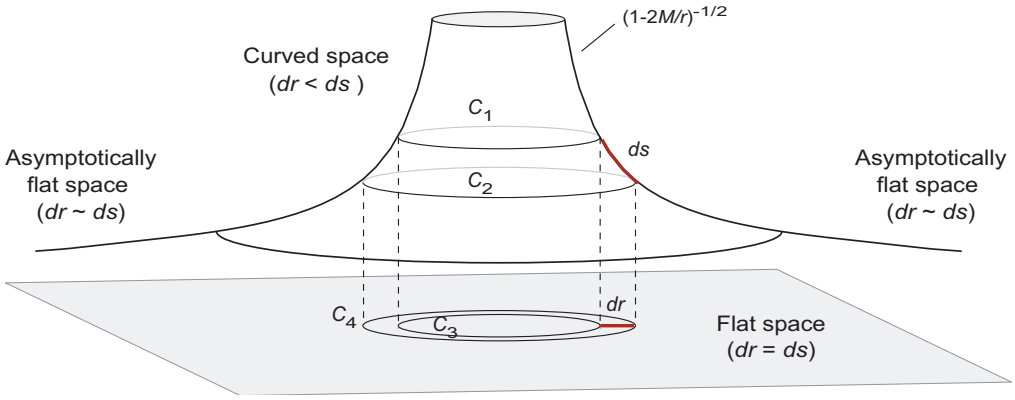

Figure 18.2: Relationship between radial coordinate distance dr and proper distance ds in Schwarzschild spacetime.

The relationship between the coordinate distance interval dr and the proper distance interval ds is illustrated further in Fig. 18.2.

- The circles C_1 and C_3 represent spheres having radius r in euclidean space.
- The circles C_2 and C_4 represent spheres having an infinitesimally larger radius $r + dr$ in euclidean space.
- In euclidean space the distance that would be measured between the spheres is dr
- But in the curved space the measured distance between the spheres is ds, which is larger than dr, by virtue of

$$ds = \frac{dr}{\sqrt{1 - \frac{2GM}{rc^2}}},$$

- Notice however that at large distances from the source of the gravitational field the Schwarzschild spacetime becomes flat and then $dr \sim ds$.

Proper and Coordinate Times

Likewise, to measure a time interval for a stationary clock at r set $dr = d\theta = d\varphi = 0$ in the line element and use $ds^2 = -d\tau^2 c^2$ to obtain

$$d\tau = \sqrt{1 - \frac{2GM}{rc^2}}\, dt.$$

- In this expression $d\tau$ is termed the *proper time* and dt is termed the *coordinate time*.
- The physical time interval measured by a local observer is given by the proper time $d\tau$, not by the coordinate time dt.
- dt and $d\tau$ coincide only if the gravitational field is weak.

Thus we see that for the gravitational field outside a spherical mass distribution

- The coordinates r and t correspond directly to *physical distance and time in Newtonian gravity*.
- In general relativity the physical (proper) distances and times must be *computed from the metric* and are *not given directly by the coordinates.*
- Only in regions of spacetime where gravity is very weak do we recover the Newtonian interpretation.

This is as it should be: *The goal of relativity is to make the laws of physics independent of the coordinate system in which they are formulated.*

The coordinates in a physical theory are like *street numbers.*

- They provide a *labeling that locates points in a space,* but knowing the street numbers is not sufficient to determine distances.
- We can't answer the question of whether the distance between 36th Street and 37th Street is the same as the distance between 40th Street and 41st Street until we know whether the streets are equally spaced.
- We must compute distances from a *metric* that gives a distance-measuring prescription.
  - Streets that are always equally spaced correspond to a "flat" space.
  - Streets with irregular spacing correspond to a position-dependent metric and thus to a "curved" space.

  For the flat space the difference in street number corresponds directly (up to a scale) to a physical distance, but in the more general (curved) case it does not.

18.1.3 Embedding Diagrams

It is sometimes useful to form a mental image of the structure for a curved space by embedding the space or a subset of its dimensions in 3-D euclidean space.

Such embedding diagrams can be misleading, as illustrated well by the case of a cylinder embedded in 3-D euclidean space, which suggests that a cylinder is curved. But it isn't:

- The cylinder is intrinsically a flat 2-D surface:
  - Cut it and roll it out into a plane, or
  - calculate its vanishing gaussian curvature.
- The cylinder has *no intrinsic curvature;* the appearance of curvature derives entirely from the embedding in 3-D space and is termed *extrinsic curvature.*

Nevertheless, the image of the cylinder embedded in 3D euclidean space is a useful representation of many properties associated with a cylinder.

We can embed only 2 dimensions of Schwarzschild spacetime in 3D euclidean space.

- Illustrate by choosing $\theta = \pi/2$ and $t = 0$, to give a 2-D metric

$$d\ell^2 = \left(1 - \frac{2M}{r}\right)^{-1} dr^2 + r^2 d\varphi^2.$$

- The metric of the 3-D embedding space is conveniently represented in cylindrical coordinates as

$$d\ell^2 = dz^2 + dr^2 + r^2 d\varphi^2$$

- This can be written on $z = z(r)$ as

$$d\ell^2 = \left(\frac{dz}{dr}\right)^2 dr^2 + dr^2 + r^2 d\varphi^2 = \left[1 + \left(\frac{dz}{dr}\right)^2\right] dr^2 + r^2 d\varphi^2$$

- Comparing

$$d\ell^2 = \left[1 + \left(\frac{dz}{dr}\right)^2\right] dr^2 + r^2 d\varphi^2 \leftrightarrow d\ell^2 = \left(1 - \frac{2M}{r}\right)^{-1} dr^2 + r^2 d\varphi^2$$

  implies that

$$z(r) = 2\sqrt{2M(r - 2M)},$$

  which defines an *embedding surface* $z(r)$ having a geometry that is the same as the Schwarzschild metric in the $(r - \varphi)$ plane.

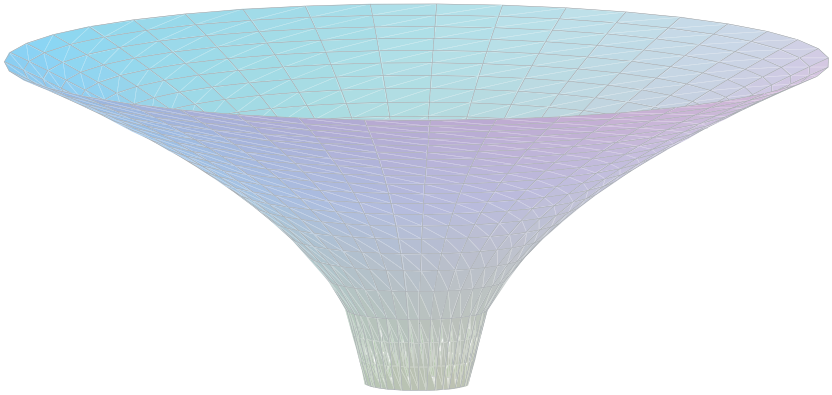

Figure 18.3: An embedding diagram for the Schwarzschild $(r-\varphi)$ plane.

Fig. 18.3 illustrates the embedding function

$$z(r) = 2\sqrt{2M(r-2M)}$$

Fig. 18.3 is not what a black hole "looks" like, but it is a striking and useful visualization of the Schwarzschild geometry. Thus such embedding diagrams are a standard representation of black holes in popular-level discussion.

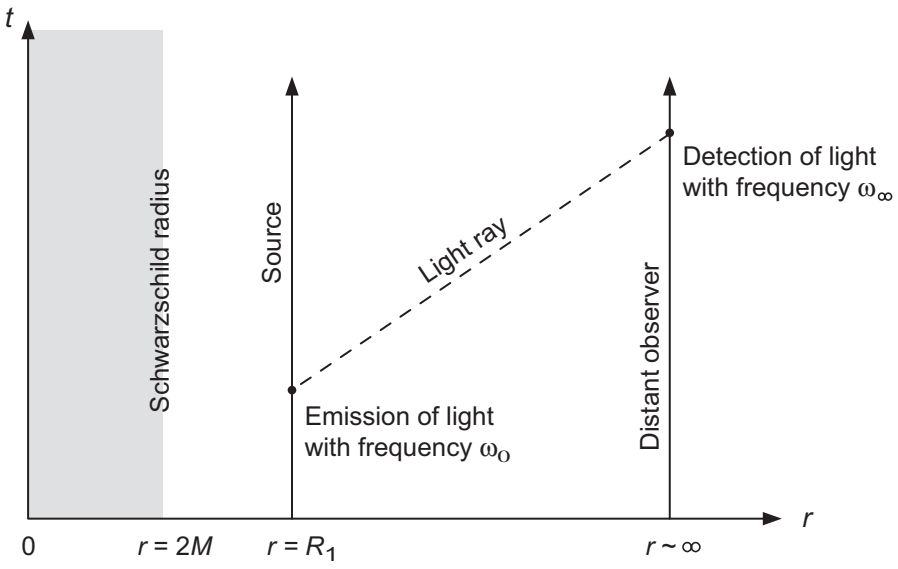

Figure 18.4: A spacetime diagram for gravitational redshift in the Schwarzschild metric.

18.1.4 The Gravitational Redshift

Emission of light from a radius R_1 that is then detected by a stationary observer at a radius $r >> R_1$ (Fig. 18.4).

For an observer with 4-velocity u, the energy measured for a photon with 4-momentum p is

$$E = \hbar\omega = -p \cdot u,$$

Observers stationary in space but not time so

$$u^i(r) = 0 \qquad u^0 \neq 0$$

Thus the 4-velocity normalization gives

$$u\cdot u = g_{\mu\nu}(x)\frac{dx^\mu}{d\tau}\frac{dx^\nu}{d\tau} = \underbrace{g_{00}(x)u^0(r)u^0(r) = -1.}_{\text{Solve for } u^0(r)}$$

and we obtain

$$u^0(r) = \sqrt{\frac{-1}{g_{00}}} = \left(1-\frac{2M}{r}\right)^{-1/2}.$$

Symmetry: Schwarzschild metric independent of time, which implies the existence of a *Killing vector*

$$\xi^\mu = (t,r,\theta,\varphi) = (1,0,0,0)$$

associated with symmetry under time displacement.

Thus, for a stationary observer at a distance r,

$$u^\mu(r) = \left(\left(1-\frac{2M}{r}\right)^{-1/2},\ 0,\ 0,\ 0\right) = \left(1-\frac{2M}{r}\right)^{-1/2}\xi^\mu.$$

The energy of the photon measured at r by stationary observer is

$$\hbar\omega(r) = -p\cdot u = -\left(1-\frac{2M}{r}\right)^{-1/2}(\xi\cdot p)_r$$

But $\xi \cdot p$ *is conserved* along the photon geodesic (ξ is a Killing vector), so $\xi \cdot p$ is in fact *independent of* r.

Therefore,

$$\hbar\omega_0 \equiv \hbar\omega(r = R_1) = -\left(1 - \frac{2M}{R_1}\right)^{-1/2} (\xi \cdot p)$$

$$\hbar\omega_\infty \equiv \hbar\omega(r \to \infty) = -(\xi \cdot p),$$

and from $\hbar\omega_\infty / \hbar\omega_0$ we obtain immediately a gravitational redshift

$$\omega_\infty = \omega_0 \left(1 - \frac{2M}{R_1}\right)^{1/2}.$$

We have made no weak-field assumptions so this result should be *valid for weak and strong fields.*

For weak fields $2M/R_1$ is small, the square root can be expanded, and the G and c factors restored to give

$$\omega_\infty \simeq \omega_0 \left(1 - \frac{GM}{R_1 c^2}\right) \qquad \text{(valid for weak fields)}$$

which is the result derived earlier using the equivalence principle.

By viewing ω as defining clock ticks, the redshift may also be interpreted as a *gravitational time dilation*.

18.1.5 Particle Orbits in the Schwarzschild Metric

Symmetries of the Schwarzschild metric:

1. Time independence → Killing vector $\xi_t = (1,0,0,0)$
2. No dependence on φ → Killing vector $\xi_\varphi = (0,0,0,1)$
3. Additional Killing vectors associated with full rotational symmetry (won't need in following).

Conserved quantities associated with these Killing vectors:

$$\varepsilon \equiv -\xi_t \cdot u = \left(1 - \frac{2M}{r}\right)\frac{dt}{d\tau}$$

$$\ell \equiv \xi_\varphi \cdot u = r^2 \sin^2\theta \frac{d\varphi}{d\tau}.$$

Physical interpretation:

- At low velocities $\ell \sim$ (orbital angular momentum / unit rest mass)
- Since $E = p^0 = mu^0 = m dt/d\tau$,

$$\lim_{r\to\infty} \varepsilon = \frac{dt}{d\tau} = \frac{E}{m}$$

  and $\varepsilon \sim$ energy / (unit rest mass) *at large distance*.

Also we have the velocity normalization constraint

$$u \cdot u = g_{\mu\nu} u^\mu u^\nu = -1.$$

The Schwarzschild line element is

$$ds^2 = -\left(1-\frac{2M}{r}\right)dt^2 + \left(1-\frac{2M}{r}\right)^{-1}dr^2 + r^2 d\theta^2 + r^2\sin^2\theta d\varphi^2$$

Conservation of angular momentum confines the particle motion to a plane, which we conveniently take to be the equatorial plane with $\theta = \frac{\pi}{2}$ implying that $d\theta = 0$, so

- $u^2 \equiv u^\theta = d\theta/d\tau = 0.$
- $\sin^2\theta = 1$

Then writing the velocity constraint

$$g_{\mu\nu}u^\mu u^\nu = -1.$$

out explicitly for the Schwarzschild metric gives

$$-\left(1-\frac{2M}{r}\right)(u^0)^2 + \left(1-\frac{2M}{r}\right)^{-1}(u^1)^2 + r^2(u^3)^2 = -1.$$

which we may rewrite using

$$u^\mu = \left(\frac{dx^0}{d\tau}, \frac{dx^1}{d\tau}, \frac{dx^2}{d\tau}, \frac{dx^3}{d\tau}\right)$$

$$\varepsilon = \left(1-\frac{2M}{r}\right)\frac{dt}{d\tau} \qquad \ell = r^2\sin^2\theta\frac{d\varphi}{d\tau}.$$

in the form

$$\frac{\varepsilon^2-1}{2} = \frac{1}{2}\left(\frac{dr}{d\tau}\right)^2 + \frac{1}{2}\left[\left(1-\frac{2M}{r}\right)\left(\frac{\ell^2}{r^2}+1\right)-1\right].$$

We can put this in the form

$$E = \frac{1}{2}\left(\frac{dr}{d\tau}\right)^2 + V_{\text{eff}}(r),$$

where we define a fictitious "energy"

$$E \equiv \frac{\varepsilon^2 - 1}{2}$$

and an effective potential

$$\begin{aligned} V_{\text{eff}}(r) &= \frac{1}{2}\left[\left(1 - \frac{2M}{r}\right)\left(\frac{\ell^2}{r^2} + 1\right) - 1\right] \\ &= \underbrace{-\frac{M}{r} + \frac{\ell^2}{2r^2}}_{\text{Newtonian}} - \underbrace{\frac{M\ell^2}{r^3}}_{\text{correction}} \end{aligned}$$

This is analogous to the energy integral of Newtonian mechanics with an effective potential V_{eff} having

- A Newtonian gravity plus centrifugal piece,
- an additional term porportional to r^{-3} that *modifies Newtonian gravity.*

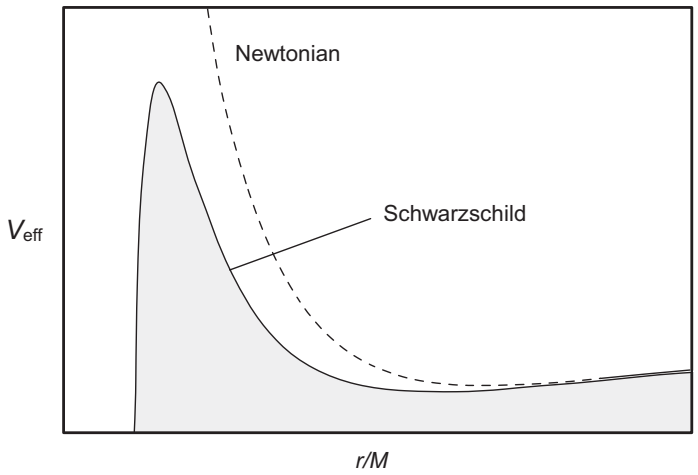

Figure 18.5: Effective potentials for finite ℓ in the Schwarzschild geometry and in Newtonian approximation.

Figure 18.5 compares the Schwarzschild effective potential with an effective Newtonian potential.

The Schwarzschild potential generally has one maximum and one minimum if $\ell/M > \sqrt{12}$.

Note the very different behavior of Schwarzschild and Newtonian mechanics at the origin because of the correction term in

$$V_{\text{eff}}(r) = \underbrace{-\frac{M}{r} + \frac{\ell^2}{2r^2}}_{\text{Newtonian}} - \underbrace{\frac{M\ell^2}{r^3}}_{\text{correction}}$$

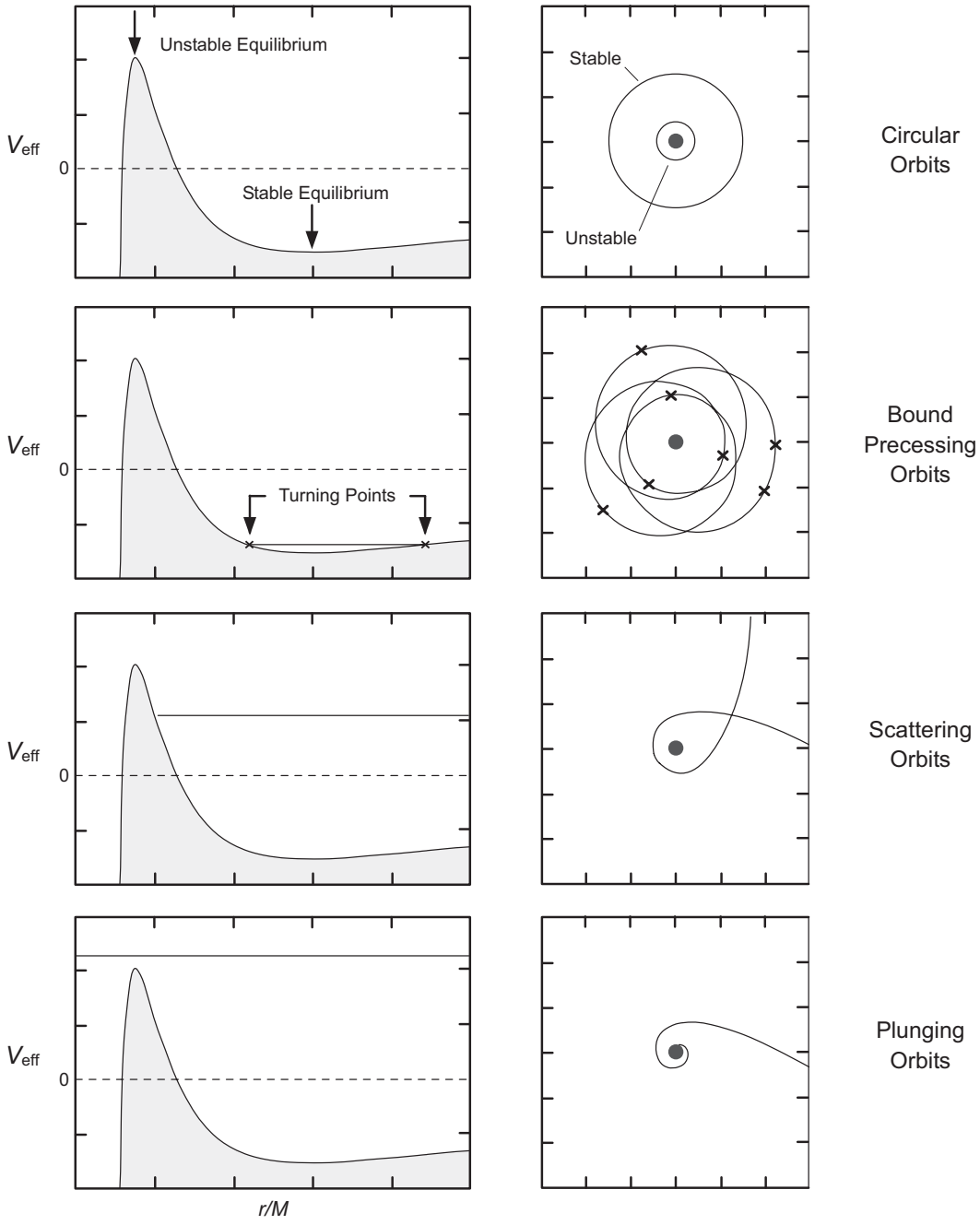

Figure 18.6: Orbits in a Schwarzschild spacetime. Effective potential on left and corresponding classes of orbits on right.

18.1.6 Innermost Stable Circular Orbit

The radial coordinate of the inner turning point for bound precessing orbits in the Schwarzschild metric is given by (Exercise)

$$r_- = \frac{\ell^2}{2M}\left(1+\sqrt{1-12\left(\frac{M}{\ell}\right)^2}\right)$$

Thus r_- has a minimum possible value when

$$\frac{M}{\ell} = \frac{1}{\sqrt{12}}.$$

The corresponding radius for the *innermost stable circular orbit* $R_{\rm ISCO}$ is then

$$R_{\rm ISCO} = 6M.$$

The innermost stable circular orbit is important in determining how much gravitational energy can be extracted from matter accreting onto neutron stars and black holes.

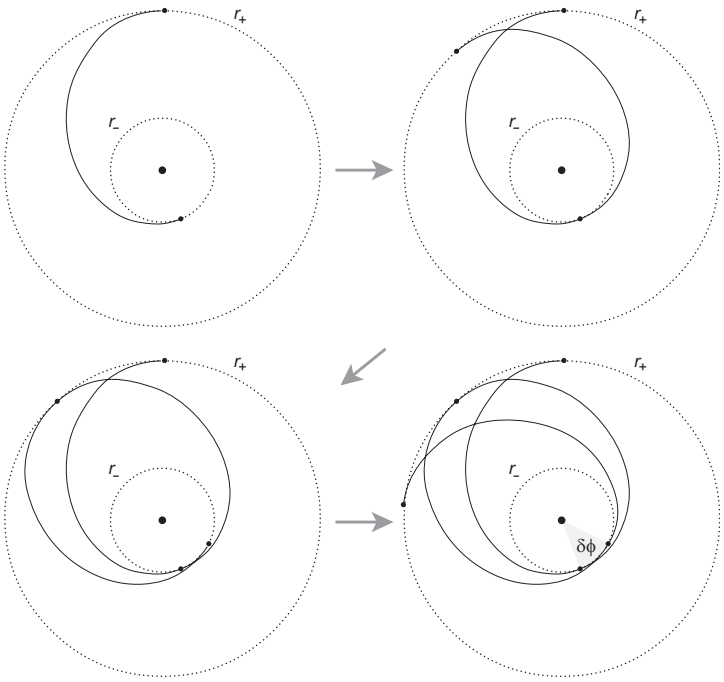

Figure 18.7: Precessing orbits in a Schwarzschild metric

18.1.7 Precession of Orbits

An orbit closes if the angle φ sweeps out exactly 2π in the passage between two successive inner or two successive outer radial turning points.

In Newtonian gravity the $1/r$ central potential → *closed elliptical orbits.* In Schwarzschild metric the effective potential deviates from $1/r$ and orbits *precess:* φ changes by more than 2π between successive radial turning points.

To investigate this precession quantitatively we require an expression for $d\varphi/dr$. From the energy equation

$$\frac{dr}{d\tau} = \pm\sqrt{2(E - V_{\text{eff}}(r))},$$

and from the conservation equation for ℓ,

$$\frac{d\varphi}{d\tau} = \frac{\ell}{r^2 \sin^2\theta}.$$

Combine, recalling that we are choosing an orbital plane $\theta = \frac{\pi}{2}$,

$$\begin{aligned}\frac{d\varphi}{dr} = \frac{d\varphi/d\tau}{dr/d\tau} &= \pm\frac{\ell}{r^2\sqrt{2(E - V_{\text{eff}}(r))}} \\ &= \pm\frac{\ell}{r^2}\left[2E - \left(1 - \frac{2M}{r}\right)\left(1 + \frac{\ell^2}{r^2}\right) + 1\right]^{-1/2} \\ &= \pm\frac{\ell}{r^2}\left[\varepsilon^2 - \left(1 - \frac{2M}{r}\right)\left(1 + \frac{\ell^2}{r^2}\right)\right]^{-1/2},\end{aligned}$$

where we have used $E = \frac{1}{2}(\varepsilon^2 - 1)$.

The change in φ per orbit, $\Delta\varphi$, can be obtained by integrating over one orbit,

$$\begin{aligned}\Delta\varphi &= \int_{r_-}^{r_+}\frac{d\varphi}{dr}\,dr + \int_{r_+}^{r_-}\frac{d\varphi}{dr}\,dr = 2\int_{r_-}^{r_+}\frac{d\varphi}{dr}\,dr \\ &= 2\ell\int_{r_-}^{r_+}\frac{dr}{r^2}\left[\varepsilon^2 - \left(1-\frac{2M}{r}\right)\left(1+\frac{\ell^2}{r^2}\right)\right]^{-1/2} \\ &= 2\ell\int_{r_-}^{r_+}\frac{dr}{r^2}\left(\underbrace{c^2(\varepsilon^2-1)+\frac{2GM}{r}-\frac{\ell^2}{r^2}}_{\text{Newtonian}} + \underbrace{\frac{2GM\ell^2}{c^2r^3}}_{\text{correction}}\right)^{-1/2}\end{aligned}$$

where in the last step G and c have been reinserted through the substitutions

$$M \to \frac{GM}{c^2} \qquad \ell \to \frac{\ell}{c},$$

Evaluation of the integral requires some care because *the integrand tends to* ∞ *at the integration limits:* From one of our earlier expressions

$$\frac{dr}{d\tau} = \pm\left[\varepsilon^2 - \left(1-\frac{2M}{r}\right)\left(1+\frac{l^2}{r^2}\right)\right]^{1/2},$$

which is the denominator of our integrand. But the limits are turning points of the radial motion and $dr/d\tau = 0$ at r_+ or r_-.

In the Solar System and most other applications the values of $\Delta\varphi$ are very small, so it is sufficient to keep only terms of order $1/c^2$ beyond the Newtonian approximation.

Expanding the integrand and evaluating the integral with due care (Exercise) yields

$$\begin{aligned}\text{Precession angle} &= \delta\varphi \equiv \Delta\varphi - 2\pi \\ &\simeq 6\pi \left(\frac{GM}{c\ell}\right)^2 \text{ rad/orbit.}\end{aligned}$$

This may be expressed in more familiar classical orbital parameters:

- In Newtonian mechanics $L = mr^2\omega$, where L is the angular momentum and ω the angular frequency.
- For Kepler orbits
$$\ell^2 = \left(\frac{L}{m}\right)^2 = \left(r^2\frac{d\varphi}{d\tau}\right)^2 \simeq \left(r^2\frac{d\varphi}{dt}\right)^2 = GMa(1-e^2),$$
where e is the eccentricity and a is the semimajor axis.

This permits us to write

$$\begin{aligned}\delta\varphi &= \frac{6\pi GM}{ac^2(1-e^2)} \\ &= 1.861\times 10^{-7}\left(\frac{M}{M_\odot}\right)\left(\frac{\text{AU}}{a}\right)\frac{1}{1-e^2} \text{ rad/orbit,}\end{aligned}$$

The form of

$$\delta\varphi = \frac{6\pi GM}{ac^2(1-e^2)}$$

shows explicitly that the amount of relativistic precession is enhanced by

- large M for the central mass,
- tight orbits (small values of a),
- large eccentricities e.

The precession observed for most objects is small.

- Precession of Mercury's orbit in the Sun's gravitational field because of general relativistic effects is observed to be *43 arcseconds per century.*
- The orbit of the Binary Pulsar precesses by about *4.2 degrees per year.*

The precise agreement of both of these observations with the predictions of general relativity is a strong test of the theory.

18.1.8 Escape Velocity in the Schwarzschild Metric

Consider a stationary observer at a Schwarzschild radial coordinate R who launches a projectile radially with a velocity v such that the projectile reaches infinity with zero velocity. This defines the escape velocity in the Schwarzschild metric.

- The projectile follows a radial geodesic since there are no forces acting on it
- The energy per unit rest mass is ε and it is conserved (time invariance of metric).
- At infinity $\varepsilon = 1$, since then the particle is at rest and the entire energy is rest mass energy. Thus $\varepsilon = 1$ at all times.

If u_{obs} is the 4-velocity of the stationary observer, the energy measured by the observer is

$$\begin{aligned} E &= -p\cdot u_{\text{obs}} = -mu\cdot u_{\text{obs}} \\ &= -mg_{\mu\nu}u^{\mu}u^{\nu}_{\text{obs}} \\ &= -mg_{00}u^{0}u^{0}_{\text{obs}} \qquad \text{(Observer stationary)}, \end{aligned}$$

where $p = mu$, with p the 4-momentum and m the rest mass, and the last step follows because the observer is stationary. But

$$\underbrace{g_{00} = -\left(1-\tfrac{2M}{r}\right)}_{\text{From metric}} \qquad \underbrace{u^{0}_{\text{obs}} = \left(1-\tfrac{2M}{R}\right)^{-1/2}}_{\text{Stationary observer}} \qquad \underbrace{u^{0} = \left(1-\tfrac{2M}{r}\right)^{-1}}_{\text{From } \varepsilon = (1-\frac{2M}{r})u^{0} = 1}$$

Therefore,

$$\begin{aligned} E &= -mg_{00}u^0u^0_{\text{obs}} \\ &= m\left(1-\tfrac{2M}{r}\right)\left(1-\tfrac{2M}{r}\right)^{-1}\left(1-\tfrac{2M}{r}\right)^{-1/2} \\ &= m\left(1-\tfrac{2M}{R}\right)^{-1/2} \end{aligned}$$

But in the observer's rest frame the energy and velocity are related by

$$E = m\gamma = m(1-v^2)^{-1/2}$$

so comparison of the two expressions for E yields

$$m\left(1-\tfrac{2M}{R}\right)^{-1/2} = m(1-v^2)^{-1/2} \quad \longrightarrow \quad v^2 = \frac{2M}{R}$$

and thus

$$v \equiv v_{\text{esc}} = \sqrt{\frac{2M}{R}}$$

Notice that

- This, coincidentally, is the same result as for Newtonian theory.
- At the Schwarzschild radius $R = r_{\text{S}} = 2M$, the escape velocity is equal to c.

This is the first hint of an *event horizon* in the Schwarzschild spacetime.

18.1.9 Radial Fall of a Test Particle in Schwarzschild Geometry

It will be instructive for later discussion to consider the particular case of a radial plunge orbit that starts from infinity with zero kinetic energy ($\varepsilon = 1$) and zero angular momentum ($\ell = 0$).

First, let us find an expression for the *proper time* as a function of the coordinate r. From earlier expressions

$$E = \frac{\varepsilon^2 - 1}{2} = \frac{1}{2}\left(\frac{dr}{d\tau}\right)^2 - \frac{M}{r} + \frac{\ell^2}{2r^2} - \frac{M\ell^2}{r^3},$$

which implies for $\ell = 0$ and $\varepsilon = 1$,

$$0 = \frac{1}{2}\left(\frac{dr}{d\tau}\right)^2 - \frac{M}{r} \quad \longrightarrow \quad \frac{dr}{d\tau} = \pm\left(\frac{2M}{r}\right)^{1/2}.$$

Choosing the negative sign (infalling orbit) and integrating with initial condition $\tau(r = 0) = 0$ gives

$$\frac{\tau}{2M} = -\frac{2}{3}\frac{r^{3/2}}{(2M)^{3/2}}$$

for the proper time τ to reach the origin as a function of the initial Schwarzschild coordinate r.

To find an expression for the *coordinate time* t as a function of r, we note that $\varepsilon = 1$ and is conserved. Then from the previous expressions

$$\varepsilon = 1 = \left(1 - \frac{2M}{r}\right)\frac{dt}{d\tau} \qquad \frac{dr}{d\tau} = \pm\left(\frac{2M}{r}\right)^{1/2}$$

we have that

$$\frac{dt}{dr} = \frac{dt/d\tau}{dr/d\tau} = -\left(1 - \frac{2M}{r}\right)^{-1}\left(\frac{2M}{r}\right)^{-1/2},$$

which may be integrated to give for the coordinate time t

$$t = 2M\left(-\frac{2}{3}\left(\frac{r}{2M}\right)^{3/2} + 2\left(\frac{r}{2M}\right)^{1/2} + \ln\left|\frac{(r/2M)^{1/2}+1}{(r/2M)^{1/2}-1}\right|\right).$$

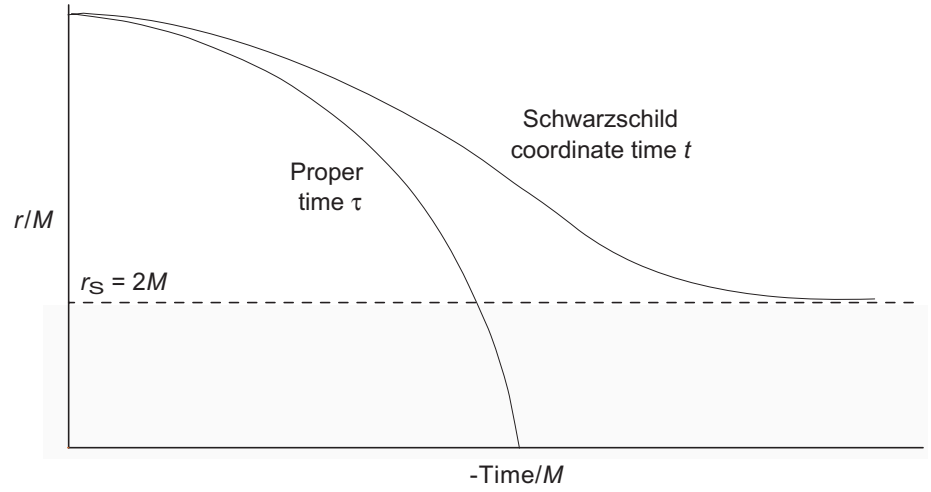

Figure 18.8: Comparison of proper time and Schwarzschild coordinate time for a particle falling radially in the Schwarzschild geometry.

The behavior of t and τ are plotted in Fig. 18.8. Notice that

- The proper time τ to fall to the origin is finite.
- For the same trajectory an infinite amount of coordinate time t elapses to reach the Schwarzschild radius.
- The smooth trajectory of the proper time through r_S suggests that the apparent singularity of the metric there is not physical.

Later in this chapter we shall introduce alternative coordinates that explicitly remove the singularity at $r = 2M$ (but not at $r = 0$).

18.1.10 Light Ray Orbits

Calculation of light ray orbits in the Schwarzschild metric largely parallels that of particle orbits, except that

$$u\cdot u = g_{\mu\nu}\frac{dx^\mu}{d\lambda}\frac{dx^\nu}{d\lambda} = 0,$$

(not $u\cdot u=-1$!) where λ is an affine parameter.

For motion in the equatorial plane $(\theta=\frac{\pi}{2})$, this becomes explicitly

$$-\left(1-\frac{2M}{r}\right)\left(\frac{dt}{d\lambda}\right)^2+\left(1-\frac{2M}{r}\right)^{-1}\left(\frac{dr}{d\lambda}\right)^2+r^2\left(\frac{d\varphi}{d\lambda}\right)^2=0.$$

By analogy with the corresponding arguments for particle motion

$$\varepsilon \equiv -\xi_t\cdot u = \left(1-\frac{2M}{r}\right)\frac{dt}{d\lambda},$$
$$\ell = \xi_\varphi\cdot u = r^2\sin^2\theta\frac{d\varphi}{d\lambda},$$

are conserved along the orbits of light rays.

With a proper choice of the normalization of the affine parameter λ, the conserved quantitity ε may be interpreted as the photon energy and the conserved quantity ℓ as its angular momentum at infinity.

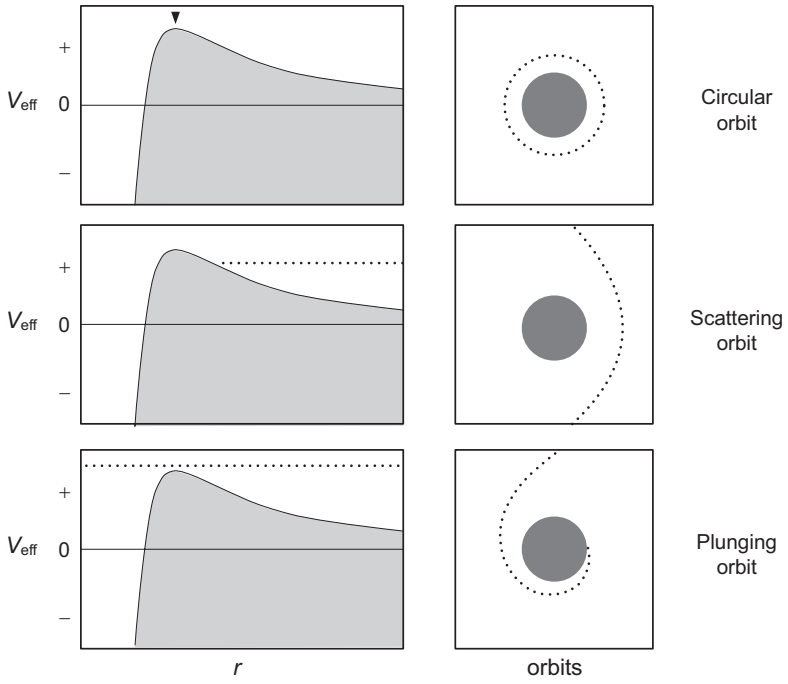

Figure 18.9: The effective potential for photons and some light ray orbits in a Schwarzschild metric. The dotted lines on the left side give the value of $1/b^2$ for each orbit.

By following steps analogous to the derivation of particle orbits

$$\frac{1}{b^2} = \frac{1}{\ell^2}\left(\frac{dr}{d\lambda}\right)^2 + V_{\text{eff}}(r)$$

$$V_{\text{eff}}(r) \equiv \frac{1}{r^2}\left(1 - \frac{2M}{r}\right) \qquad b^2 \equiv \frac{\ell^2}{\varepsilon^2}.$$

The effective potential for photons and some classes of light ray orbits in the Schwarzschild geometry are illustrated in Fig. 18.9.

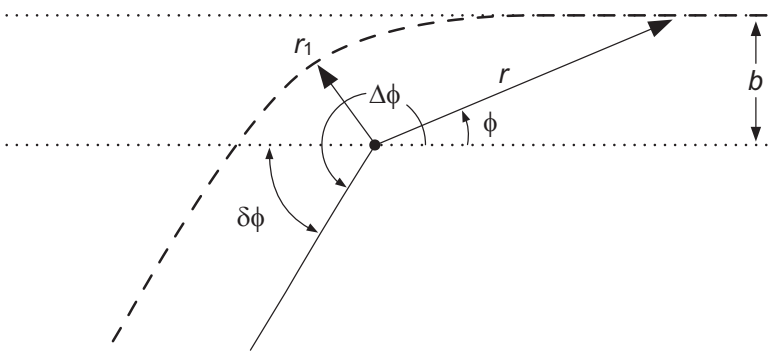

Figure 18.10: Deflection of light by an angle $\delta\varphi$ in a Schwarzschild metric.

18.1.11 Deflection of Light in a Gravitational Field

Proceeding in a manner similar to that for the calculation of the precession angle for orbits of massive objects, we may calculate the deflection $d\varphi/dr$ for a light ray in the Schwarzschild metric.

The result is

$$\delta\varphi = \frac{4GM}{c^2 b} = 2.970 \times 10^{-28} \left(\frac{M}{\text{g}}\right)\left(\frac{\text{cm}}{b}\right) \text{ radians}$$
$$= 8.488 \times 10^{-6} \left(\frac{M}{M_\odot}\right)\left(\frac{R_\odot}{b}\right) \text{ radians.}$$

For a photon grazing the surface of the Sun, $M = 1\,M_\odot$ and $b = 1\,R_\odot$, which gives $\delta\varphi \simeq 1.75$ arcseconds.

Observation of this deflection during a total solar eclipse catapulted Einstein to worldwide fame almost overnight in the early 1920s.

18.2 Schwarzschild Black Holes

There is an event horizon in the Schwarzschild spacetime at $r_S = 2M$, which implies a black hole inside the event horizon (escape velocity exceeds c).

Place analysis on firmer ground by considering a spacecraft approaching the event horizon in free fall (engines off).

- For simplicity, we assume the trajectory to be radial.
- Consider from two points of view
  1. From a very distant point at constant distance from the black hole (professors sipping martinis).
  2. From a point inside the spacecraft (students).
- Use the Schwarzschild solution (metric) for analysis.

18.2.1 Approaching the Event Horizon: Outside View

We consider only *radial motion.* Setting $d\theta = d\varphi = 0$ in the line element gives

$$\begin{aligned} ds^2 &= -d\tau^2 \\ &= -\left(1-\frac{2M}{r}\right)dt^2 + \left(1-\frac{2M}{r}\right)^{-1}dr^2 + r^2\underbrace{d\theta^2}_{=0} + r^2\sin^2\theta\,\underbrace{d\varphi^2}_{=0} \\ &= -\left(1-\frac{2M}{r}\right)dt^2 + \left(1-\frac{2M}{r}\right)^{-1}dr^2 \\ &= -\left(1-\frac{r_S}{r}\right)dt^2 + \left(1-\frac{r_S}{r}\right)^{-1}dr^2. \end{aligned}$$

- As the spacecraft approaches the event horizon its velocity as viewed from far outside in a fixed frame is $v = dr/dt$.
- Light signals from spacecraft travel on the light cone ($ds^2 = 0$) and thus from the line element

$$ds^2 = 0 = -\left(1-\frac{r_S}{r}\right)dt^2 + \left(1-\frac{r_S}{r}\right)^{-1}dr^2$$

Solve for $\frac{dr}{dt}$ to give

$$v \equiv \frac{dr}{dt} = \left(1-\frac{r_S}{r}\right).$$

- As viewed from a distance outside r_S, *the spacecraft appears to slow as it approaches r_S and eventually stops as $r \to r_S$.*
- Thus, from the exterior we would never see the spacecraft cross r_S: *its image would remain frozen at $r = r_S$ for all eternity.*

But let us examine what this means a little more carefully. Rewrite

$$\frac{dr}{dt} = \left(1 - \frac{r_S}{r}\right) \quad \rightarrow \quad dt = \frac{dr}{1 - r_S/r}.$$

- As $r \rightarrow r_S$ time between successive wave crests for the light wave coming from the spacecraft tends to infinity and therefore

$$\lambda \rightarrow \infty \qquad \nu \rightarrow 0 \qquad E \rightarrow 0.$$

- The external observer not only sees the spacecraft slow rapidly as it approaches r_S, but the spacecraft image is observed to *strongly redshift* at the same time.
- This behavior is just that of the coordinate time already seen for a test particle in radial free fall:

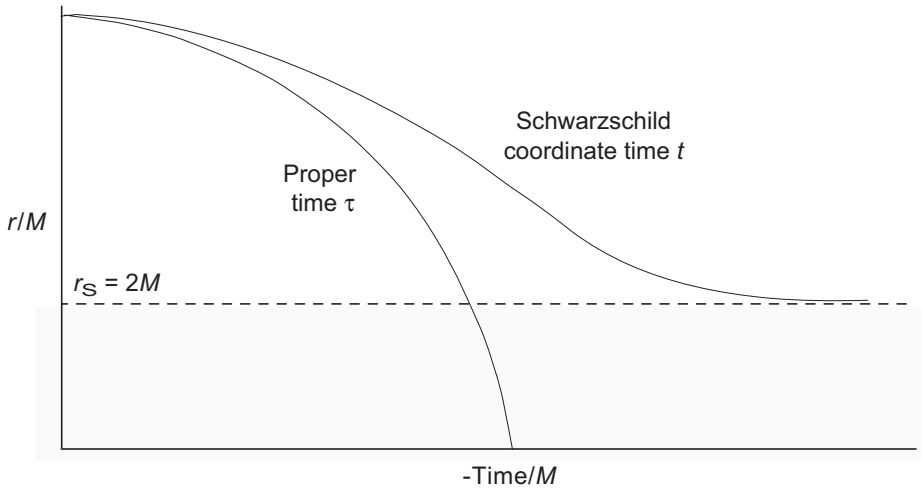

- Therefore, more properly, the external observation is that *the spacecraft approaching r_S rapidly slows and redshifts until the image fades from view before the spacecraft reaches r_S.*

18.2.2 Approaching the Event Horizon: Spacecraft View

Things are very different as viewed by the (doomed) students from the interior of the spacecraft.

- The occupants will use their own clocks (*measuring proper time*) to gauge the passage of time.
- Starting from a radial position r_0 outside the event horizon, the spacecraft will reach the origin in a proper time

$$\tau = -\frac{2}{3}\frac{r_0^{3/2}}{(2M)^{1/2}}.$$

- The spacecraft occupants will generally notice *no spacetime singularity at the horizon.*
- Any tidal forces at the horizon may be very large but will remain finite (*Riemann curvature is finite at the Schwarzschild radius*).
- The spacecraft crosses r_s and reaches the (real) singularity at $r = 0$ in a finite amount of time, where it would encounter infinite tidal forces (*Riemann curvature has components that become infinite at the origin*).
- The trip from r_s to the singularity is very fast (Exercise):
  1. Of order 10^{-4} seconds for stellar-mass black holes.
  2. Of order 10 minutes for a billion solar mass black hole.

18.2.3 Lightcone Description of a Trip to a Black Hole

It is highly instructive to consider a lightcone description of a trip into a Schwarzschild black hole. First we consider the region outside the Schwarzschild radius.

- Assuming *radial light rays*

$$\underbrace{d\theta = d\varphi}_{\text{radial}} = \underbrace{ds^2}_{\text{light}} = 0$$

  the line element reduces to

$$ds^2 = -\left(1 - \frac{2M}{r}\right) dt^2 + \left(1 - \frac{2M}{r}\right)^{-1} dr^2 = 0,$$

- Thus the *equation for the lightcone* at some local coordinate r in the Schwarzschild metric can be read directly from the metric

$$\frac{dt}{dr} = \pm \left(1 - \frac{2M}{r}\right)^{-1}.$$

  where

  - The plus sign corresponds to outgoing photons (r increasing with time for $r > 2M$)
  - The minus sign to ingoing photons (r decreasing with time for $r > 2M$)

- For $r \to \infty$

$$\frac{dt}{dr} = \pm \left(1 - \frac{2M}{r}\right)^{-1}.$$

  becomes equal to ± 1, as for flat spacetime.

- However as $r \to r_s$ the forward lightcone opening angle tends to zero because $dt/dr \to \infty$.

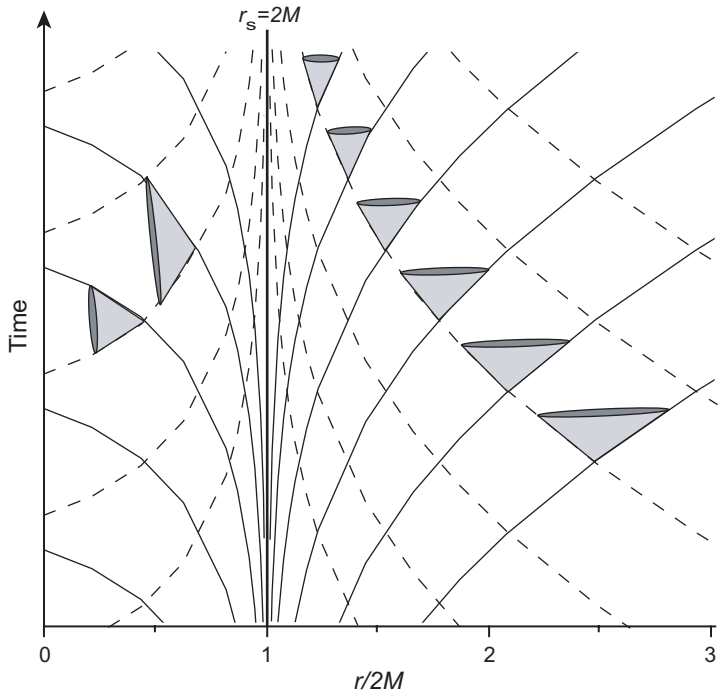

Figure 18.11: Photon paths and lightcone structure of the Schwarzschild spacetime.

Integrating

$$\frac{dt}{dr} = \pm\left(1 - \frac{2M}{r}\right)^{-1}.$$

gives

$$t = \begin{cases} -r - 2M\ln|r-1| + \text{ constant} & \text{(Ingoing)} \\ r + 2M\ln|r-1| + \text{ constant} & \text{(Outgoing)} \end{cases}$$

- The null geodesics defined by this expression are plotted in Fig. 18.11.
- The tangents at the intersections of the dashed and solid lines define local lightcones corresponding to dt/dr, which are sketched at some representative spacetime points.

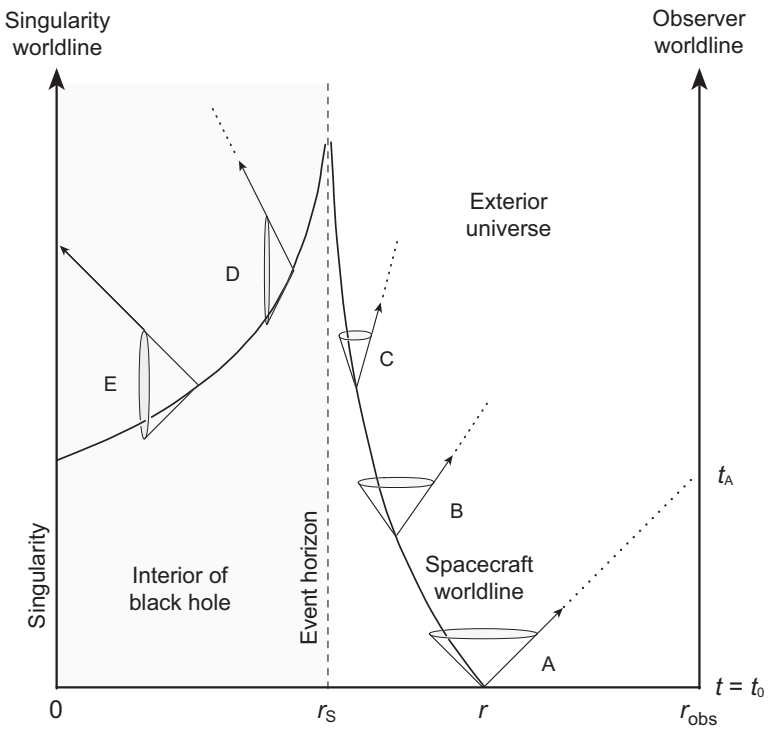

Figure 18.12: Light cone description of a trip into a Schwarzschild black hole.

- The worldline of a spacecraft is illustrated in Fig. 18.12, starting well exterior to the black hole. The gravitational field there is weak and the light cone has the usual symmetric appearance.
- As illustrated by the dotted line from A, a light signal emitted from the spacecraft can intersect the worldline of an observer remaining at constant distance $r_{\rm obs}$ at a finite time $t_{\rm A} > t_0$.
- As the spacecraft falls toward the black hole on the worldline indicated the forward light cone begins to narrow since

$$\frac{dt}{dr} = \pm\left(1 - \frac{2M}{r}\right)^{-1}.$$

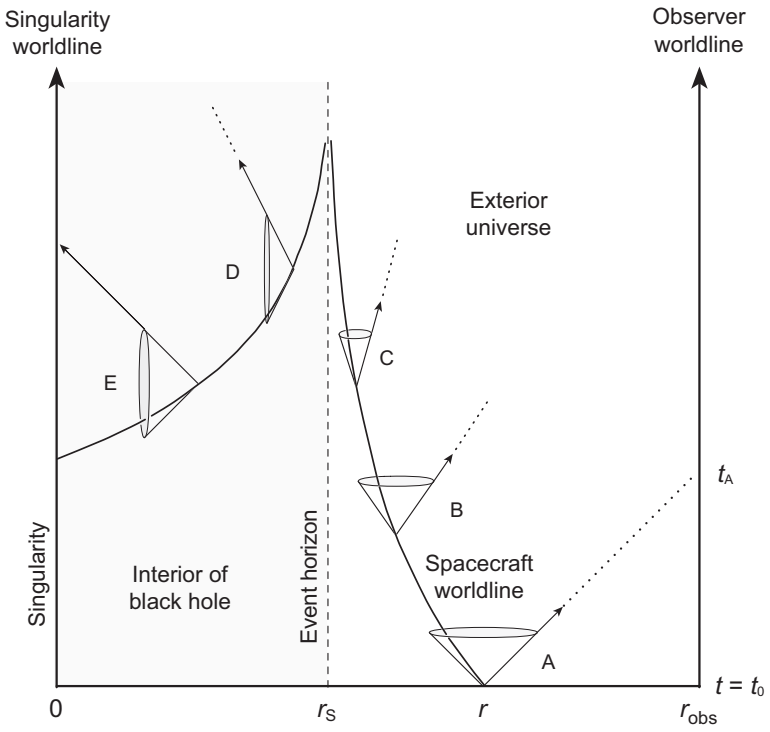

- Now, at B a light signal can intersect the external observer worldline only at a distant point in the future (arrow on light cone B).
- As the spacecraft approaches r_S, the opening angle of the forward light cone tends to zero and a signal emitted from the spacecraft tends toward *infinite time* to reach the external observer's worldline at r_{obs} (arrow on light cone C).
- *The external observer sees infinite redshift as the spacecraft approaches the Schwarzschild radius.*

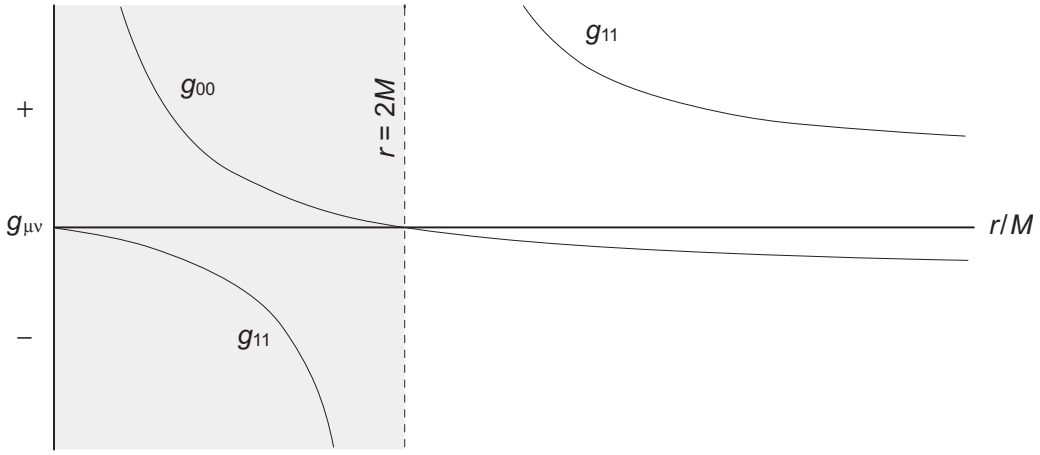

Figure 18.13: Spacelike and timelike regions for g_{00} and g_{11} in the Schwarzschild metric.

Now consider light cones *interior to the Schwarzschild radius.*

- From the structure of the radial and time parts of the Schwarzschild metric illustrated in Fig. 18.13, we observe that *dr and dt reverse their character at the horizon* ($r = 2M$) because the metric coefficients g_{00} and g_{11} *switch signs* at that point.

  1. Outside the event horizon the t direction, $\partial/\partial t$, is timelike ($g_{00} < 0$) and the r direction, $\partial/\partial r$, is spacelike ($g_{11} > 0$).
  2. Inside the event horizon, $\partial/\partial t$ is spacelike ($g_{00} > 0$) and $\partial/\partial r$ is timelike ($g_{11} < 0$).

- Thus inside the event horizon the lightcones get rotated by $\pi/2$ relative to outside (space $\leftrightarrow$ time).

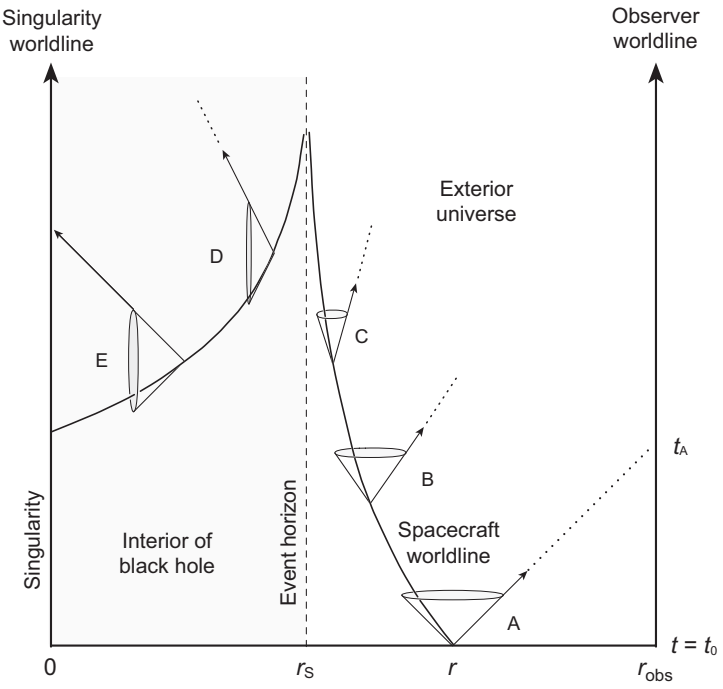

- The worldline of the spacecraft descends inside r_S because the coordinate time decreases (it is now behaving like r) and the decrease in r represents the passage of time, but the *proper time* is continuously increasing in this region.
- Outside the horizon r is a *spacelike coordinate* and application of enough rocket power can reverse the infall and make r begin to increase.
- Inside the horizon r is a *timelike coordinate* and no application of rocket power can reverse the direction of time.
- Thus, the radial coordinate of the spacecraft must decrease once inside the horizon, for the same reason that time flows into the future in normal experience (whatever that reason is!).

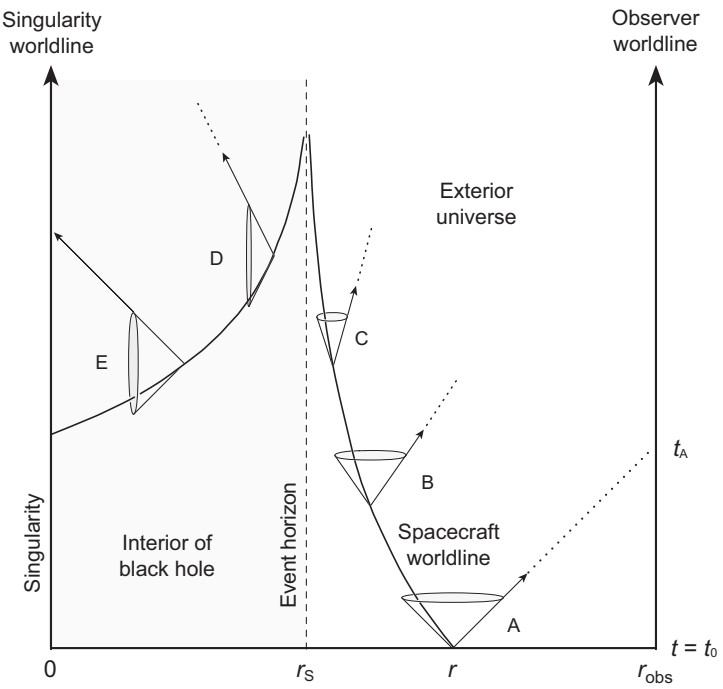

- Inside the horizon there are no paths in the forward light cone of the spacecraft that can reach the external observer at r_0 (the right vertical axis)—see the light cones labeled D and E.

> All timelike and null paths inside the horizon are bounded by the horizon and must encounter the singularity at $r = 0$.

- This illustrates succinctly the real reason that nothing can escape the interior of a black hole. *Dynamics (building a better rocket) are irrelevant:* once inside r_s the geometry of spacetime permits
  - no forward light cones that intersect exterior regions, and
  - no forward light cones that can avoid the origin.

Spacetime geometry is destiny; resistance is futile!

Thus, there is no escape from the classical Schwarzschild black hole because

1. There are literally no paths in spacetime that go from the interior to the exterior.
2. All timelike or null paths within the horizon lead to the singularity at $r = 0$.

But notice the adjective "classical" . . . More later.

The preceding discussion is illuminating but the interpretation of the results is complicated by the behavior near the coordinate singularity at $r = 2M$.

- We now discuss alternative coordinate systems that remove the coordinate singularity at the horizon.
- Although these coordinate systems have advantages for interpreting the interior behavior of the Schwarzschild geometry, the standard coordinates remain useful for describing the exterior behavior because of their simple asymptotic behavior.

18.2.4 Eddington–Finkelstein Coordinates

In the *Eddington–Finkelstein coordinate system* a new variable v is introduced through

$$t = \underbrace{v}_{\text{new}} - r - 2M \ln \left| \frac{r}{2M} - 1 \right|,$$

where r, t, and M have their usual meanings in the Schwarzschild metric, and θ and φ are assumed to be unchanged. For either $r > 2M$ or $r < 2M$, insertion into the standard Schwarzschild line element gives (Exercise)

$$ds^2 = -\left(1 - \frac{2M}{r}\right) dv^2 + 2dvdr + r^2 d\theta^2 + r^2 \sin^2\theta d\varphi^2.$$

- The Schwarzschild metric expressed in these new coordinates

$$ds^2 = -\left(1 - \frac{2M}{r}\right) dv^2 + 2dvdr + r^2 d\theta^2 + r^2 \sin^2\theta d\varphi^2.$$

  is manifestly non-singular at $r = 2M$

- The singularity at $r = 0$ remains.
- Thus the singularity at the Schwarzschild radius is a coordinate singularity that can be removed by a new choice of coordinates.

Let us consider behavior of radial light rays expressed in these coordinates.

- Set $d\theta = d\varphi = 0$ (radial motion)
- Set $ds^2 = 0$ (light rays).

Then the Eddington–Finkelstein line element gives

$$-\left(1 - \frac{2M}{r}\right) dv^2 + 2dvdr = 0.$$

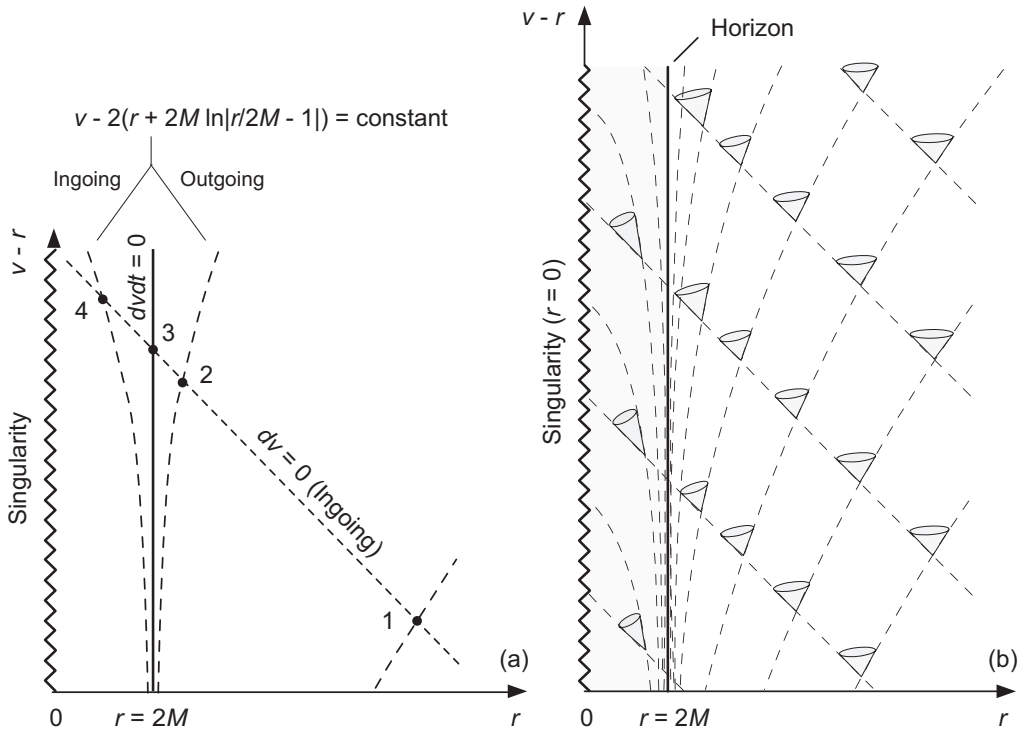

Figure 18.14: (a) Eddington–Finkelstein coordinates for the Schwarzschild black hole with r on the horizontal axis and $v - r$ on the vertical axis. Only two coordinates are plotted, so each point corresponds to a 2-sphere of angular coordinates. (b) Light cones in Eddington–Finkelstein coordinates.

This equation has two general solutions and one special solution [see Fig. 18.14(a)]:

$$-\left(1-\frac{2M}{r}\right)dv^2+2dvdr=0.$$

- *General Solution 1:* $dv = 0$, so $v =$ constant. $\rightarrow$ Ingoing light rays on trajectories of constant v (dashed lines Fig. 18.14(a)) .

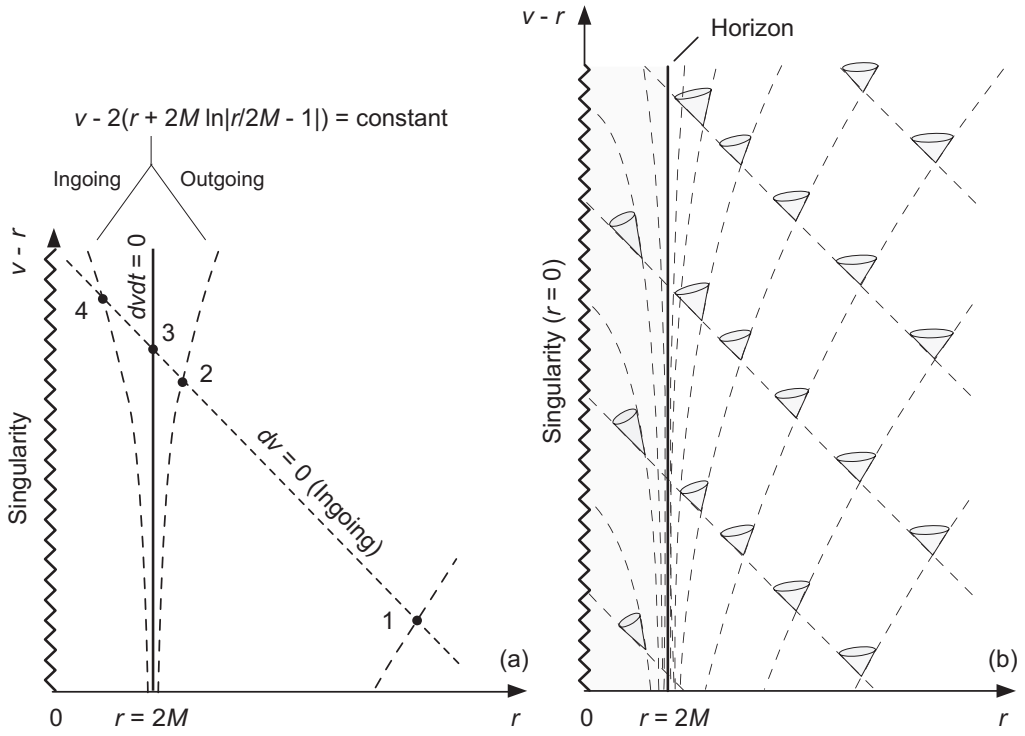

- *General Solution 2:* If $dv \neq 0$, then divide by dv^2 to give

$$-\left(1-\frac{2M}{r}\right)dv^2 + 2dvdr = 0 \quad \rightarrow \quad \frac{dv}{dr} = 2\left(1-\frac{2M}{r}\right)^{-1},$$

which yields upon integration

$$v - 2\left(r + 2M\ln\left|\frac{r}{2M}-1\right|\right) = \text{ constant}.$$

This solution changes behavior at $r = 2M$:

1. Outgoing for $r > 2M$.
2. Ingoing for $r < 2M$ (r decreases as v increases).

The long-dashed curves in Fig. 18.14(a) illustrate both ingoing and outgoing world-lines corresponding to this solution.

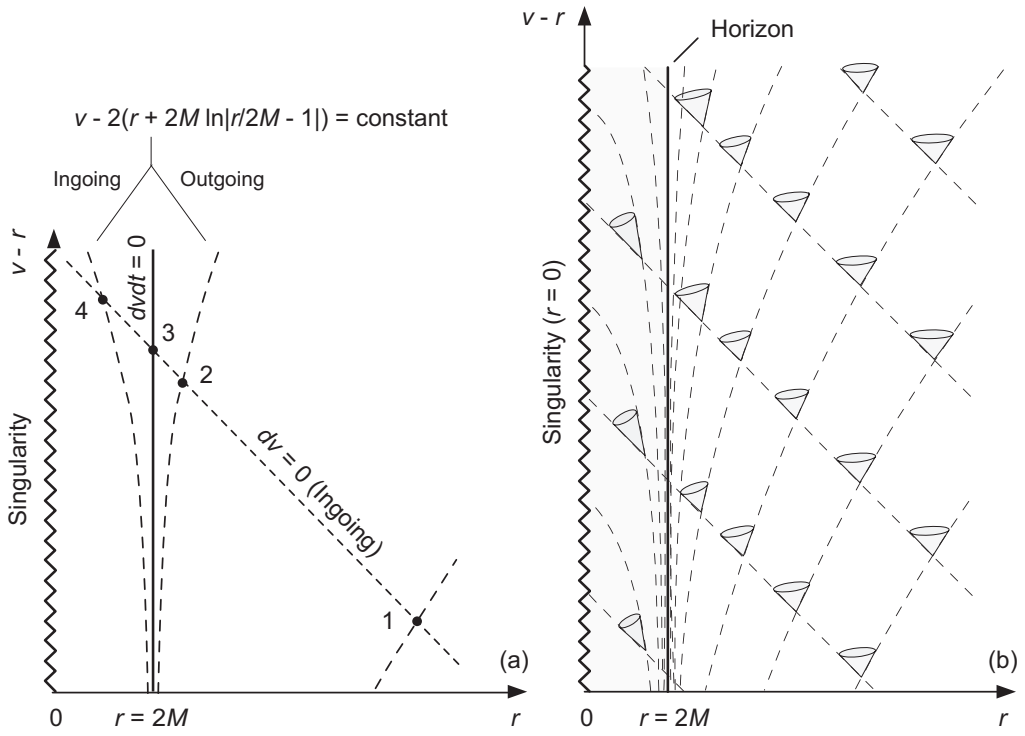

- *Special Solution:* In the special case that $r = 2M$, the differential equation reduces to

$$-\left(1-\frac{2M}{r}\right)dv^2 + 2dvdr = 0 \quad \rightarrow \quad dvdr = 0,$$

which corresponds to light trapped at the Schwarzschild radius. The vertical solid line at $r = 2M$ represents this solution.

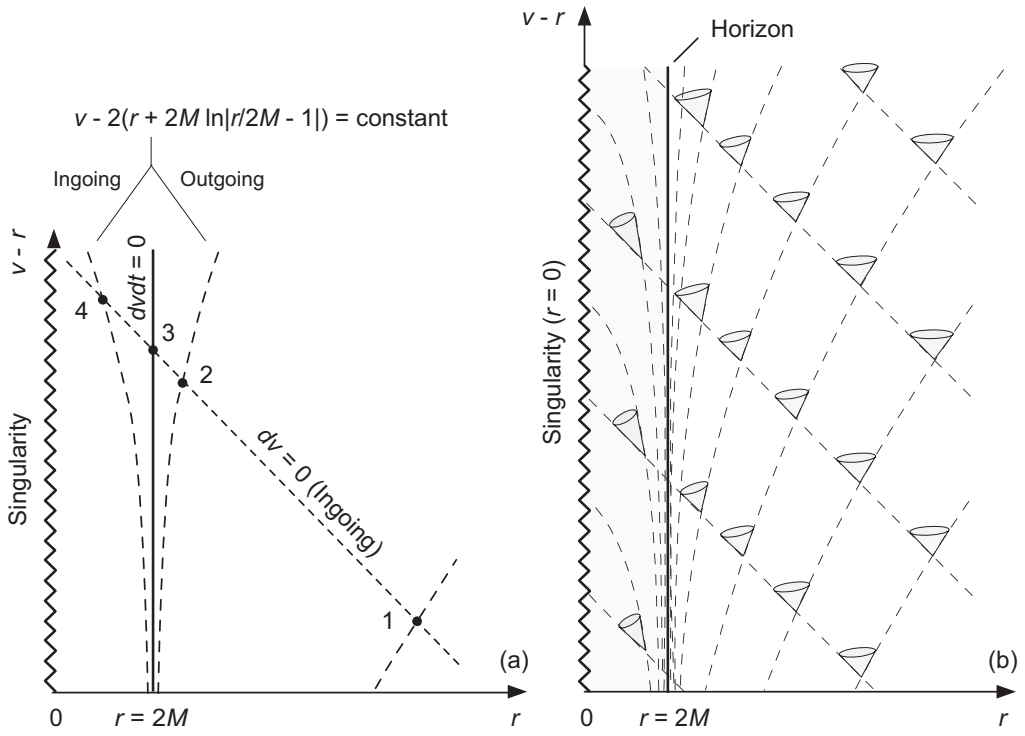

For every spacetime point in Fig. 18.14(a) there are two solutions.

- For the points labeled 1 and 2 these correspond to an ingoing and outgoing solution.
- For point 3 one solution is ingoing and one corresponds to light trapped at $r = r_S$.
- For point 4 both solutions are ingoing.

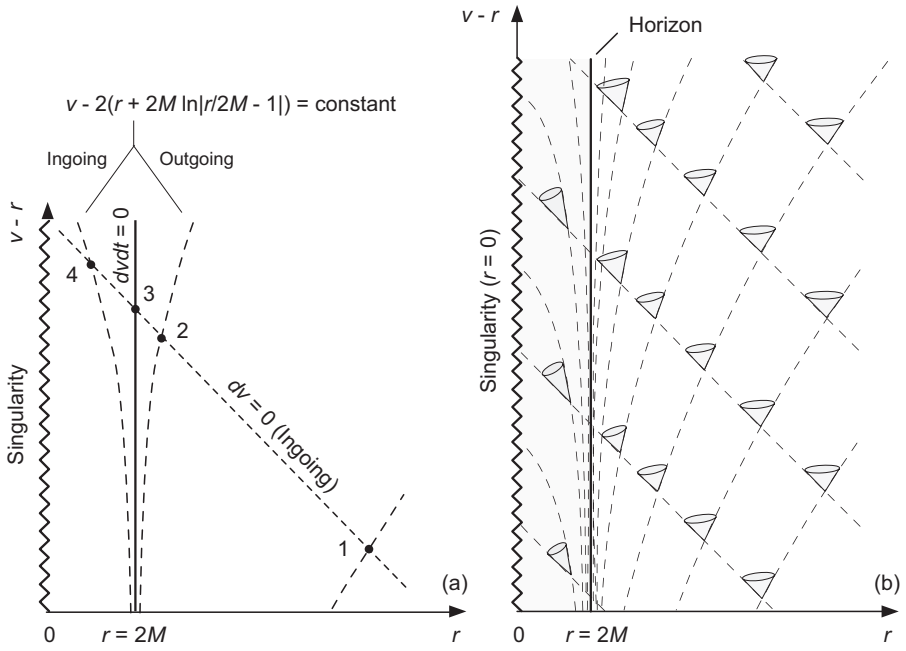

The two solutions passing through a point determine the light cone structure at that point (right side of figure).

- The light cones at various points are bounded by the two solutions, so they tilt "inward" as r decreases.
- The radial light ray that defines the left side of the light cone is ingoing (general solution 1).
- If $r \neq 2M$, the radial light ray defining the right side of the light cone corresponds to general solution 2.
    1. These propagate outward if $r > 2M$.
    2. For $r < 2M$ they propagate *inward*.
- For $r < 2M$ the light cone is tilted sufficiently that no light ray can escape the singularity at $r = 0$.
- At $r = 2M$, one light ray moves inward; one is trapped at $r = 2M$.

The horizon may be viewed as a null surface generated by the radial light rays that can neither escape to infinity nor fall in to the singularity.

18.2.5 Kruskal–Szekeres Coordinates

The *Kruskal–Szekeres coordinates* exhibit no singularity at the Schwarzschild radius $r = 2M$.

- Introduce variables (v, u, θ, φ), where θ and φ have their usual meaning and the new variables u and v are defined through

$$\begin{aligned} u &= \left(\frac{r}{2M} - 1\right)^{1/2} e^{r/4M} \cosh\left(\frac{t}{4M}\right) \qquad (r > 2M) \\ &= \left(1 - \frac{r}{2M}\right)^{1/2} e^{r/4M} \sinh\left(\frac{t}{4M}\right) \qquad (r < 2M) \\ v &= \left(\frac{r}{2M} - 1\right)^{1/2} e^{r/4M} \sinh\left(\frac{t}{4M}\right) \qquad (r > 2M) \\ &= \left(1 - \frac{r}{2M}\right)^{1/2} e^{r/4M} \cosh\left(\frac{t}{4M}\right) \qquad (r < 2M) \end{aligned}$$

- The corresponding line element is

$$ds^2 = \frac{32M^3}{r} e^{-r/2M}(-dv^2 + du^2) + r^2 d\theta^2 + r^2 \sin^2\theta\, d\varphi^2,$$

  where $r = r(u, v)$ is defined through

$$\left(\frac{r}{2M} - 1\right) e^{r/2M} = u^2 - v^2.$$

- This metric is manifestly non-singular at $r = 2M$, but singular at $r = 0$.

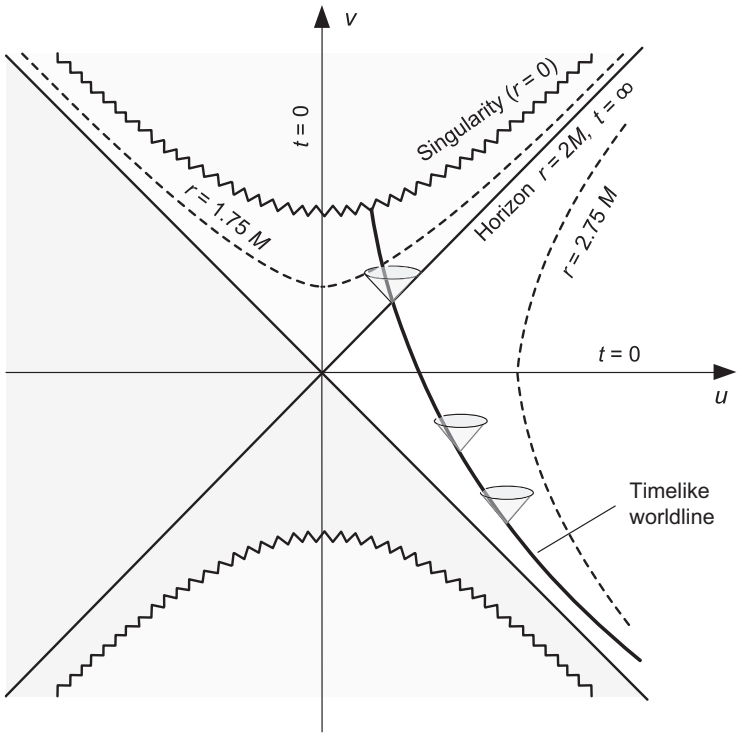

Figure 18.15: Kruskal–Szekeres coordinates. Only the two coordinates u and v are displayed; each point is really a 2-sphere in the variables θ and φ.

Kruskal diagram: lines of constant r and t plotted on a u and v grid. Figure 18.15 illustrates.

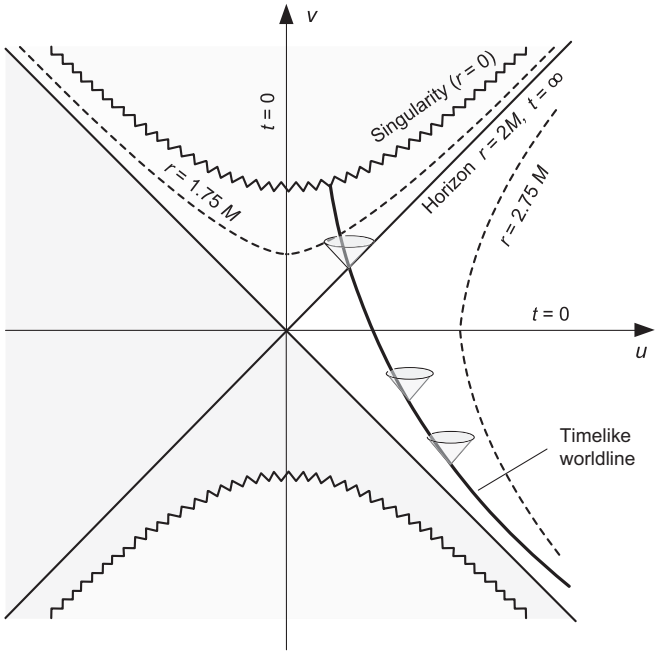

- From the form of

$$\left(\frac{r}{2M}-1\right)e^{r/2M}=u^2-v^2.$$

  lines of constant r are *hyperbolae of constant* u^2-v^2.

- From the definitions of u and v

$$\begin{aligned} v &= u\tanh\left(\frac{t}{4M}\right) && (r>2M)\\ &= \frac{u}{\tanh\left(t/4M\right)} && (r<2M). \end{aligned}$$

  Thus, lines of constant t are straight lines with slope

  - $\tanh(t/4M)$ for $r>2M$
  - $1/\tanh(t/4M)$ for $r<2M$.

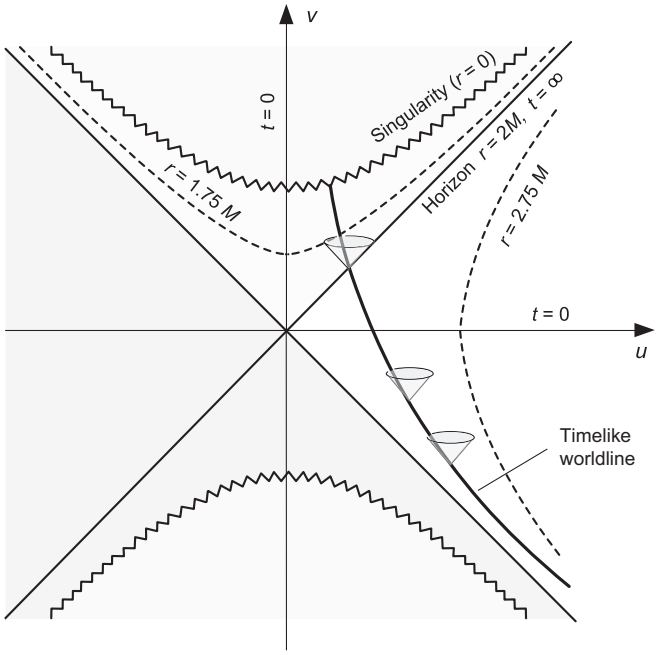

- For radial light rays in Kruskal–Szekeres coordinates ($d\theta = d\varphi = ds^2 = 0$), and the line element

$$ds^2 = \frac{32M^3}{r} e^{-r/2M}(-dv^2 + du^2) + r^2 d\theta^2 + r^2 \sin^2\theta d\varphi^2$$

yields

$$dv = \pm du$$

> 45 degree lightcones in the uv parameters, just like flat space.

- Over the full range of Kruskal–Szekeres coordinates (v, u, θ, φ), the metric component $g_{00} = g_{vv}$ remains negative and $g_{11} = g_{uu}$, $g_{22} = g_{\theta\theta}$, and $g_{33} = g_{\varphi\varphi}$ remain positive.
- Therefore, the v direction is *always timelike* and the u direction is *always spacelike*, in contrast to the normal Schwarzschild coordinates where r and t switch their character at the horizon.

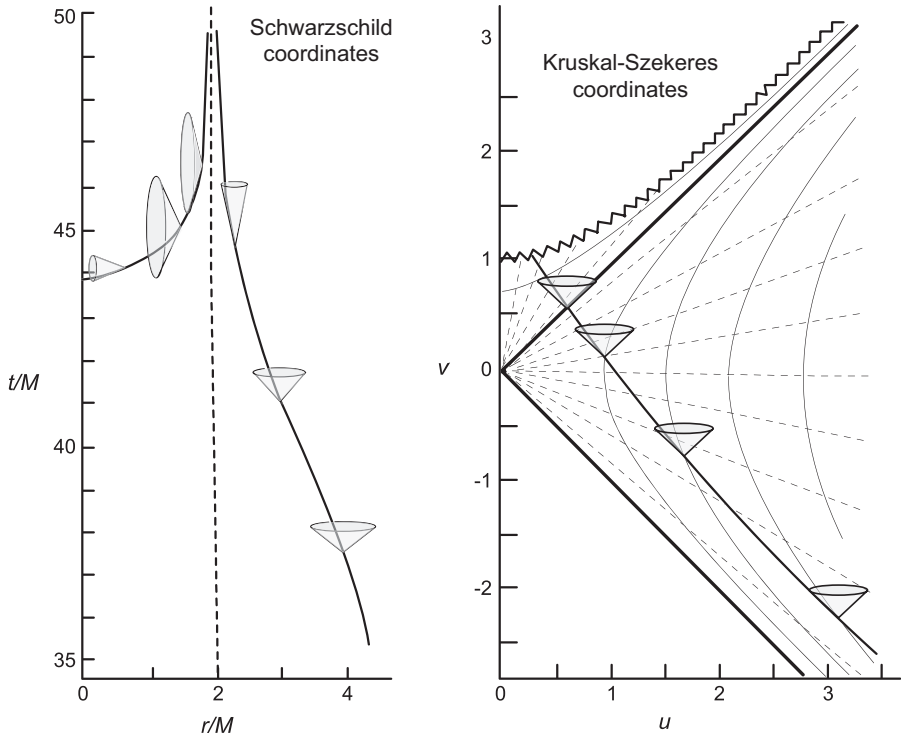

Figure 18.16: A trip to the center of a black hole in standard Schwarzschild coordinates and in Kruskal–Szekeres coordinates.

The identification of $r = 2M$ as an event horizon is particularly clear in Kruskal–Szekeres coordinates (Fig. 18.16).

- The light cones make 45-degree angles with the vertical and the horizon also makes a 45-degree angle with the vertical.
- Thus, for any point within the horizon, its forward worldline *must* contain the $r = 0$ singularity and *cannot* contain the $r = 2M$ horizon.

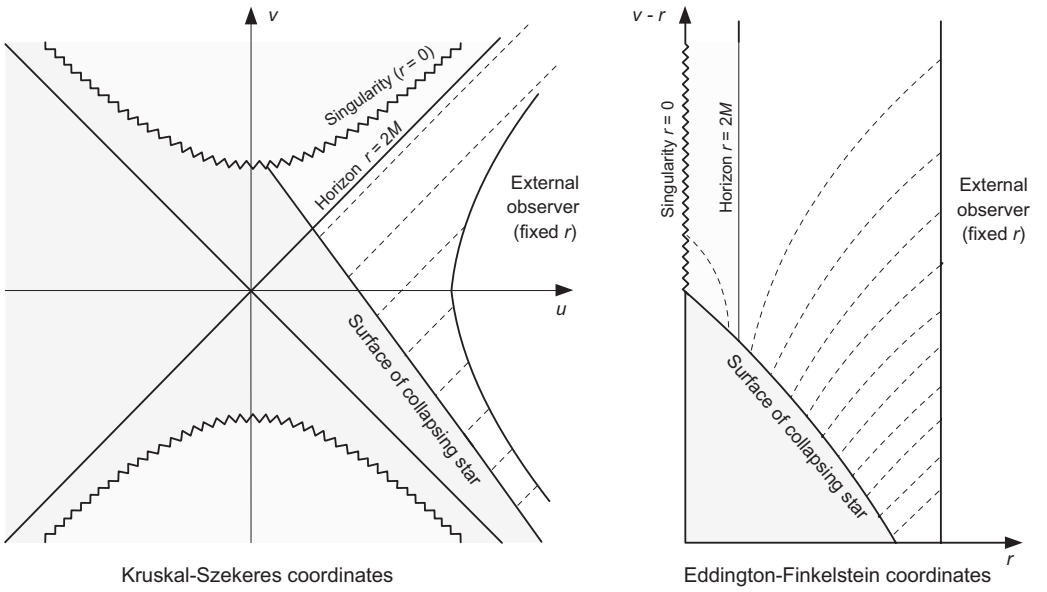

Figure 18.17: Collapse to a Schwarzschild black hole.

Figure 18.17 illustrates a spherical mass distribution (a star, for example) collapsing to a black hole as represented in Kruskal–Szekeres coordinates and in Eddington–Finkelstein coordinates.

- A distant observer remains at fixed r (hyperbola) and observes periodic light signals sent from the surface of the collapsing star.
- Light pulses, propagating on the dashed lines, arrive at longer and longer intervals as measured by the outside observer.
- At the horizon, light signals take an infinite length of time to reach the external observer.
- Once the surface is inside the horizon, no signals can reach the outside observer and the entire star collapses to the singularity.
- Note: the Schwarzschild solution is valid only *outside* the star. Inside GR applies but the solution is not Schwarzschild.

18.3 Hawking Black Holes: Black Holes Are Not Really Black!

Classically, the fundamental structure of curved spacetime ensures that nothing can escape from within the Schwarzschild event horizon. That is an emphatically *deterministic* statement. But what about quantum mechanics, which is fundamentally *indeterminate*?

18.3.1 Deterministic Geodesics and Quantum Uncertainty

- Our discussion to this point has been classical in that it assumes that free particles follow geodesics appropriate for the spacetime.
- But the uncertainty principle implies that microscopic particles cannot be completely localized on classical trajectories because they are subject to a spatial coordinate and 3-momentum uncertainty of the form $\Delta p_i \Delta x_i \geq \bar{h}$;
- Neither can energy conservation be imposed except with an uncertainty $\Delta E \Delta t \geq \bar{h}$, where ΔE is an energy uncertainty and Δt is the corresponding time period during which this energy uncertainty
- This implies an inherent *quantum fuzziness* in the 4-momenta associated with our description of spacetime at the quantum level.

For the Killing vector $\xi \equiv \xi_t = (1,0,0,0)$ in the Schwarzschild metric,

$$\xi\cdot\xi = g_{\mu\nu}\xi^\mu\xi^\nu = g_{00}\xi^0\xi^0 = \underbrace{-\left(1-\frac{2M}{r}\right)}_{\text{changes sign at } r_s} ,$$

from which we conclude that

ξ is $\begin{cases} \textit{timelike outside the horizon,} \text{ since then } \xi\cdot\xi < 0, \\ \textit{spacelike inside the horizon,} \text{ since then } \xi\cdot\xi > 0. \end{cases}$

As we now make plausible, this property of the Killing vector ξ

- permits a virtual quantum fluctuation of the vacuum to be converted into real particles, and
- these particles are detectable at infinity as emission of mass from the black hole.

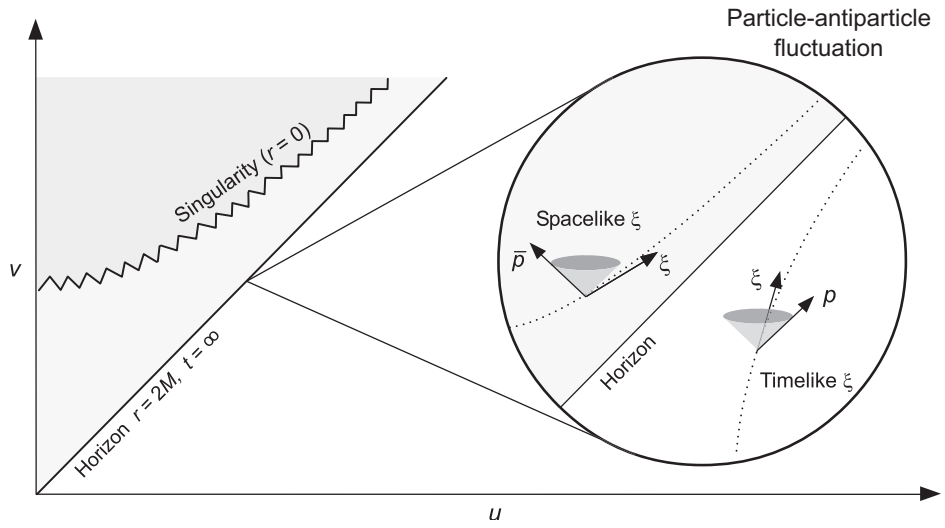

Figure 18.18: Hawking radiation in Kruskal–Szekeres coordinates.

18.3.2 Hawking Radiation

Assume a particle–antiparticle pair created by vacuum fluctuation near the horizon of a Schwarzschild black hole, such that the particle and antiparticle end up on opposite sides of the horizon (Fig. 18.18).

- If the particle–antiparticle pair is created in a small enough region of spacetime, there is nothing special implied by this region lying at the event horizon: the spacetime is indistinguishable from Minkowski space because of the equivalence principle.
- Therefore, the normal principles of (special) relativistic quantum field theory will be applicable to the pair creation process in a local inertial frame defined at the event horizon (even if the gravitational field is enormous there).

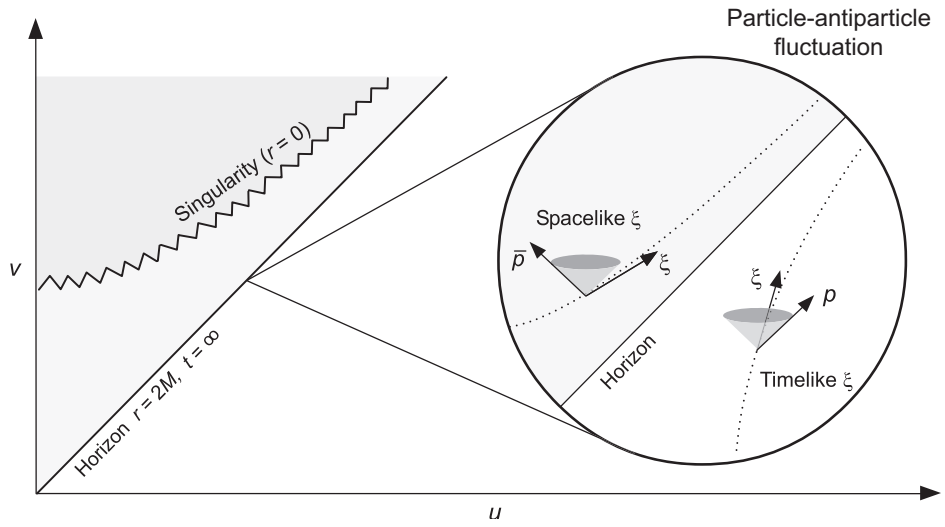

- In the Schwarzschild geometry, the conserved quantity analogous to the total energy in flat space is the scalar product of the Killing vector $\xi \equiv \xi_t = (1,0,0,0)$ with the 4-momentum p.
- Therefore, if a particle–antiparticle pair is produced near the horizon with 4-momenta p and $\bar{p}$, respectively, the condition

$$\xi \cdot p + \xi \cdot \bar{p} = 0,$$

  must be satisfied (to preserve vacuum quantum numbers).
- *For the particle outside the horizon,* $-\xi \cdot p > 0$ (it is proportional to an energy that is measureable externally).
- *If the antiparticle were also outside the horizon,* it too *must* have $-\xi \cdot \bar{p} > 0$, in which case
  1. The condition $\xi \cdot p + \xi \cdot \bar{p} = 0$ *cannot be satisfied.*
  2. The particle–antiparticle pair can have only a fleeting existence of duration $\Delta t \sim \hbar/\Delta E$ (Heisenberg).
- So far, no surprises . . .

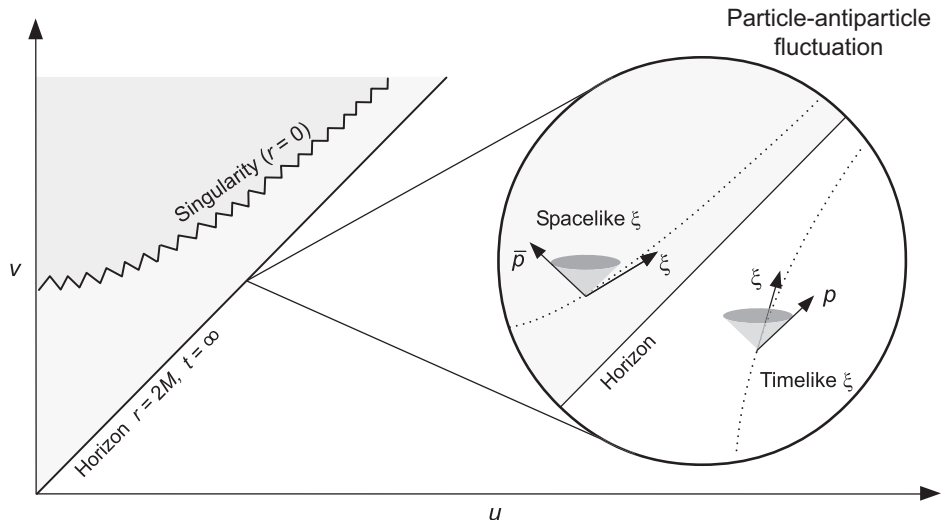

HOWEVER . . .

If instead (as in the figure) the antiparticle is *inside the horizon,*

- The Killing vector ξ is *spacelike* ($\xi \cdot \xi > 0$)
- The scalar product $-\xi \cdot \bar{p}$ is *not an energy* (for any observer)
- In fact, the product $-\xi \cdot \bar{p}$ is a *3-momentum component*.
- Therefore $-\xi \cdot \bar{p}$ can be *positive or negative (!!).*

There is magic afoot:

- If $-\xi \cdot \bar{p}$ is negative, then $\xi \cdot p + \xi \cdot \bar{p} = 0$ *can be satisfied.*
- Then the virtual particle created outside the horizon can propagate to infinity as a *real, detectable particle,* while the antiparticle remains trapped inside the event horizon.
- The black hole *emits its mass as a steady stream of particles (!).*

Therefore, quantum effects imply that a black hole can emit its mass as a flux of particles and antiparticles created through vacuum fluctuations near its event horizon. The emitted particles are termed *Hawking radiation*.

The Hawking mechanism has been described by loose analogy with a rather nefarious financial transaction.

- Suppose that I am broke (a money vacuum), but I wish to give to you a large sum of money (in Euros, E).
- Next door is a bank—*Uncertainty Bank and Trust*—that has lots of money in its secure vault but has shoddy lending practices. Then

1. I borrow a large sum of money ΔE from the Uncertainty Bank, which will take a finite time Δt to find that I have no means of repayment.

> We hypothesize $\Delta E \cdot \Delta t \sim h$, where h is constant, since the bank will be more diligent if the amount of money is larger.

2. I transfer the money ΔE to your account.
3. I declare bankruptcy within the time Δt, leaving the bank on the hook for the loan.

A virtual fluctuation of the money vacuum has caused real money to be emitted (and detected in your distant account!) from behind the seemingly impregnable event horizon of the bank vault.

18.3.3 Mass Emission Rates and Black Hole Temperature

The methods for obtaining quantitative results from the Hawking theory are beyond our scope, but the results can be stated simply:

- The rate of mass emission can be calculated using relativistic quantum field theory:

$$\frac{dM}{dt} = -\lambda \frac{\hbar}{M^2},$$

  where λ is a dimensionless constant.

- The distribution of energies emitted in the form of Hawking radiation is equivalent to a *blackbody with temperature*

$$T = \frac{\hbar c^3}{8\pi k_B G M} = 6.2 \times 10^{-8} \left(\frac{M_\odot}{M}\right) \text{ K}.$$

  Advanced methods of quantum field theory are required to prove this, but there are suggestive hints from the observations that

  1. A black hole acts as a perfect absorber of radiation (as would a blackbody).
  2. Hawking radiation originates in random fluctuations, as we would expect for a thermal emission process.

- Integrating $dM/dt = -\lambda\hbar/M^2$ for a black hole assumed to emit all of its mass by Hawking radiation in a time t_H, we obtain

$$M(t) = (3\lambda\hbar(t_H - t))^{1/3}$$

  for its mass as a function of time.

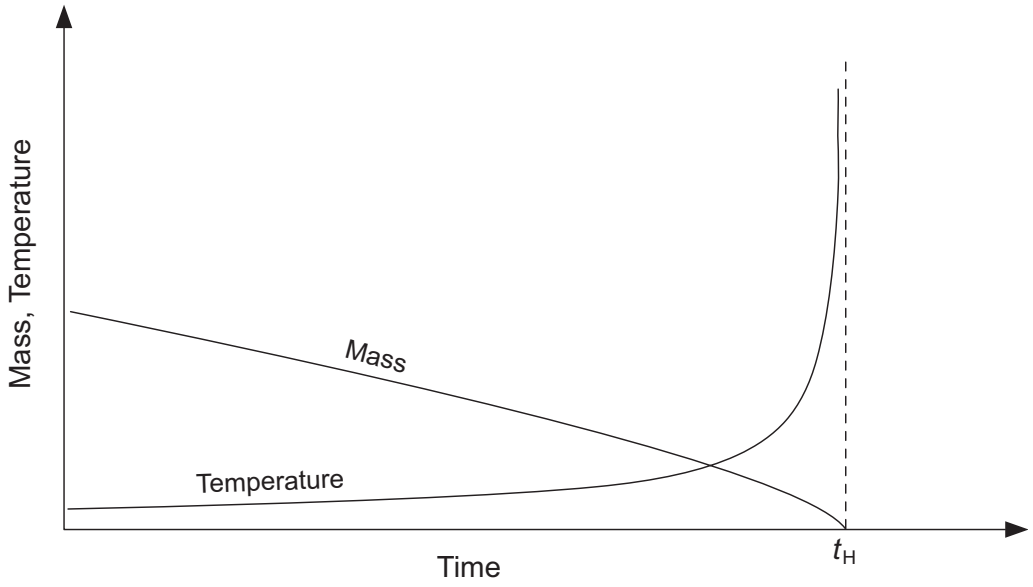

Figure 18.19: Evaporation of a Hawking black hole.

From the results

$$T = \frac{\hbar c^3}{8\pi k_B G M} \qquad \frac{dM}{dt} = -\lambda \frac{\hbar}{M^2} \qquad M(t) = (3\lambda\hbar(t_H - t))^{1/3}$$

the mass and temperature of the black hole behave as in Fig. 18.19. Therefore,

- The black hole evaporates at an accelerating rate as it loses mass.
- Both the temperature and emission rate of the black hole tend to infinity near the end.
- Observationally we may expect a final burst of very high energy (gamma-ray) radiation that would be characteristic of Hawking evaporation for a black hole.

18.3.4 Miniature Black Holes

How long does it take a black hole to evaporate by the quantum Hawking process? From the mass emission rate formula we may estimate a lifetime for complete evaporation as

$$M(t) = (3\lambda\hbar(t_{\rm H} - t))^{1/3} \quad \rightarrow \quad t_{\rm H} \simeq \frac{M^3}{3\lambda\hbar} \simeq 10^{-25}\left(\frac{M}{1\text{g}}\right)^3 \text{ s.}$$

- A one solar mass black hole would then take approximately 10^{53} times the present age of the Universe to evaporate (with a corresponding blackbody temperature of order 10^{-7} K). *It's pretty black!*
- However, black holes of initial mass $\sim 10^{14}$ g or less would have evaporation lifetimes less than or equal to the present age of the Universe, and their demise could be detectable through a characteristic burst of high-energy radiation.
- The Schwarzschild radius for a 10^{14} g black hole is approximately 1.5×10^{-14} cm, which is about $\frac{1}{5}$ *the size of a proton.* To form such a black hole one must compress 10^{14} grams (mass of a large mountain) into a volume less than the size of a proton!
- Early in the big bang there could have been such densities. Therefore, a population of miniature black holes could have formed in the big bang and could be decaying in the present Universe with a detectable signature.
- No experimental evidence has yet been found for such miniature black holes and their associated Hawking radiation. (They would have to be relatively nearby to be seen easily.)

18.3.5 Black Hole Thermodynamics

The preceding results suggest that the gravitational physics of black holes and classical thermodynamics are closely related. Remarkably, this has turned out to be correct.

- It had been noted prior to Hawking's discovery that there were similarities between black holes and black body radiators.
- The difficulty with describing a black hole in thermodynamical terms was that a classical black hole permits no equilibrium with the surroundings *(it absorbs but cannot emit radiation)*.
- Hawking radiation supplies the necessary equilibrium that ultimately allows thermodynamics and a temperature to be ascribed to a black hole.

Hawking Area Theorem: If A is the surface area (area of the event horizon) for a black hole, Hawking proved a theorem that A *cannot decrease* in any physical process involving a black hole horizon,

$$\frac{dA}{dt} \geq 0.$$

- For a Schwarzschild black hole, the horizon area is

$$A = 16\pi M^2 \quad \longrightarrow \quad \frac{dA}{dM} = 32\pi M,$$

which can be written ($h =$ Planck, $k_B =$ Boltzmann).

$$dM = \frac{1}{32\pi M}\, dA \quad \longrightarrow \quad dM = \frac{h}{8\pi k_B M}\, d\left(\frac{k_B A}{4h}\right)$$

- But $dE = dM$ is the change in total energy and the temperature of the black hole is $T = \hbar/8\pi k_B M$ in $c = G = 1$ units.

- Therefore, we may write the preceding as

$$\underbrace{dE = T\,dS}_{\text{1st Law}} \qquad \underbrace{dS \geq 0}_{\text{2nd Law}} \qquad \underbrace{S \equiv \frac{k_B}{4h} A}_{\text{entropy}}$$

which are just the 1st and 2nd laws of thermodynamics if

$$S \propto \text{ (surface area (!) of the black hole)}$$

is interpreted as entropy!

Evaporation of a black hole through Hawking radiation appears to violate the Hawking area theorem in that the black hole eventually disappears. However,

- The area theorem assumes that a local observer always measures positive energy densities and that there are no spacelike energy fluxes.
- As far as is known these are correct assumptions at the classical level, but they may break down in quantum processes.
- The correct quantum interpretation of Hawking radiation and the area theorem is that
  1. The entropy of the evaporating, isolated black hole *decreases* with time (because it is proportional to the area of the horizon).
  2. The total entropy of the Universe *increases* because of the entropy associated with the Hawking radiation itself.
  3. That is, the area theorem is replaced by

Generalized 2nd Law: The total entropy of the black hole plus exterior Universe may never decrease in any process.

18.3.6 Gravity and Quantum Mechanics: the Planck Scale

The preceding results for Hawking radiation are derived assuming that the spacetime in which the quantum calculations are done is a fixed background that is not influenced by the propagation of the Hawking radiation.

- This approximation is expected to be valid as long as $E << M$, where E is the average energy of the Hawking radiation and M is the mass of the black hole.
- This approximation breaks down on a scale given by the *Planck mass*

$$M_{\rm P} = \left(\frac{\hbar c}{G}\right)^{1/2} = 1.2 \times 10^{19}\ {\rm GeV\ c^{-2}} = 2.2 \times 10^{-8}\ {\rm kg}.$$

- For a black hole of this mass, the effects of gravity become important even on a quantum ($\hbar$) scale, requiring a theory of *quantum gravity*.
- We don't yet have an adequate theory of quantum gravity.
- Note that near the endpoint of Hawking black hole evaporation one approaches the Planck scale.
- Therefore, we do not actually know yet what happens at the conclusion of Hawking evaporation for a black hole.

18.4 The Kerr Solution: Rotating Black Holes

The Schwarzschild solution corresponds to the simplest black hole, which can be characterized by a single parameter, the mass M.

- Other solutions to the field equations of general relativity permit black holes with more degrees of freedom.

> The most general black hole can possess
>
> 1. Mass
> 2. Charge
> 3. Angular momentum
>
> as distinguishing quantities.

- Of particular interest are those solutions where we relax the restriction to spherical symmetry and thus permit the black hole to be characterized by angular momentum in addition to mass (*Kerr black holes*).
- Rotating black holes are of particular interest in astrophysics because they are thought to power
  - quasars and other active galaxies,
  - X-ray binaries, and
  - gamma-ray bursts.
- Unlike for Schwarzschild black holes, *energy and angular momentum can be extracted* from a (classical) rotating black hole.

18.4.1 The Kerr Metric

The Kerr metric corresponds to the line element

$$ds^2 = -\left(1 - \frac{2Mr}{\rho^2}\right) dt^2 - \frac{4Mra\sin^2\theta}{\rho^2} d\varphi dt + \frac{\rho^2}{\Delta} dr^2 + \rho^2 d\theta^2 + \left(r^2 + a^2 + \frac{2Mra^2\sin^2\theta}{\rho^2}\right) \sin^2\theta d\varphi^2$$

with the definitions

$$a \equiv J/M \qquad \rho^2 \equiv r^2 + a^2\cos^2\theta \qquad \Delta \equiv r^2 - 2Mr + a^2.$$

- The coordinates (t, r, θ, φ) are called *Boyer–Lindquist coordinates*.
- The parameter a, termed the *Kerr parameter,* has units of length in geometrized units.
- The parameter J will be interpreted as angular momentum and the parameter M as the mass for the black hole.

The Kerr line element

$$ds^2 = -\left(1 - \frac{2Mr}{\rho^2}\right) dt^2 - \frac{4Mra\sin^2\theta}{\rho^2} d\varphi dt + \frac{\rho^2}{\Delta} dr^2 + \rho^2 d\theta^2 + \left(r^2 + a^2 + \frac{2Mra^2\sin^2\theta}{\rho^2}\right) \sin^2\theta d\varphi^2$$

$$a \equiv J/M \qquad \rho^2 \equiv r^2 + a^2\cos^2\theta \qquad \Delta \equiv r^2 - 2Mr + a^2.$$

has the following properties.

- *Vacuum solution:* the Kerr metric is a vacuum solution of the Einstein equations, valid in the absence of matter.
- *Reduction to Schwarzschild metric:* If the black hole is not rotating ($a = J/M = 0$), the Kerr line element reduces to the Schwarzschild line element.
- *Asymptotically flat:* The Kerr metric becomes asymptotically flat for $r >> M$ and $r >> a$.
- *Symmetries:* The Kerr metric is independent of t and φ, implying the existence of Killing vectors

  $$\xi_t = (1,0,0,0) \qquad \text{(stationary metric)}$$
  $$\xi_\varphi = (0,0,0,1) \qquad \text{(axially symmetric metric).}$$

  Unlike the Schwarzschild metric, the Kerr metric has only axial symmetry.
- The metric has off-diagonal terms

  $$g_{03} = g_{30} = -\frac{2Mra\sin^2\theta}{\rho^2} \qquad \text{(inertial frame dragging).}$$

For the Kerr line element

$$ds^2 = -\left(1 - \frac{2Mr}{\rho^2}\right) dt^2 - \frac{4Mra\sin^2\theta}{\rho^2} d\varphi dt + \frac{\rho^2}{\Delta} dr^2 + \rho^2 d\theta^2 + \left(r^2 + a^2 + \frac{2Mra^2\sin^2\theta}{\rho^2}\right) \sin^2\theta d\varphi^2$$

$$a \equiv J/M \qquad \rho^2 \equiv r^2 + a^2\cos^2\theta \qquad \Delta \equiv r^2 - 2Mr + a^2.$$

- Surfaces of constant Boyer–Lindquist coordinates r and t do not have the metric of a 2-sphere.
- *Singularity and horizon structure:* $\Delta \to 0$ at

  $$r_\pm = M \pm \sqrt{M^2 - a^2}$$

  and $ds \to \infty$, assuming $a \leq M$.

  1. This is a coordinate singularity.
  2. As $a \to 0$ we find that $r_+ \to 2M$, which coincides with the Schwarzschild coordinate singularity.
  3. Thus r_+ *corresponds to the horizon* that makes the Kerr solution a black hole.

  On the other hand, the limit $\rho \to 0$ corresponds to a *physical singularity* with associated infinite components of spacetime curvature, similar to the case for the Schwarzschild solution.

18.4.2 Extreme Kerr Black Holes

- The horizon radius

$$r_{\pm} = M \pm \sqrt{M^2 - a^2}$$

  exists only for $a \leq M$.

- Thus, there is a maximum angular momentum $J_{\max}$ for a Kerr black hole since $a = J/M$ and $a_{\max} = M$,

$$J_{\max} = a_{\max} M = M^2.$$

- Black holes for which $J = M^2$ are termed *extreme Kerr black holes.*

- Near-extreme black holes may develop in many astrophysical situations:

  1. Angular momentum transfer through accretion disks in either binary systems or around supermassive black holes in galaxy cores tends to spin up the central object.
  2. Massive stars collapsing to black holes may have significant initial angular momentum

18.4.3 Cosmic Censorship

That the horizon exists for a Kerr black hole only under restricted conditions raises the question of whether a singularity could exist in the absence of a horizon (*"naked singularity"*).

Cosmic Censorship Hypothesis: Nature conspires to "censor" spacetime singularities in that *all such singularities come with event horizons* that render them invisible to the outside universe.

- No known violations (observationally or theoretically).
- It cannot at this point be derived from any more fundamental concept and must be viewed as only an hypothesis.
- All theoretical attempts to add angular momentum to a Kerr black hole in order to cause it to exceed the maximum angular momentum permissable for existence of the horizon have failed.

18.4.4 The Kerr Horizon

The area of the horizon for a black hole is of considerable importance because of the area theorem, which states that the horizon area of a classical black hole can never decrease in any physical process.

- The Kerr horizon corresponds to a constant value of $r = r_+$.
- Since the metric is stationary, the horizon is also a surface of constant t.
- Setting $dr = dt = 0$ in the Kerr line element gives the *line element for the 2-D horizon*,

$$d\sigma^2 = \rho_+^2 d\theta^2 + \left(\frac{2Mr_+}{\rho_+}\right)^2 \sin^2\theta d\varphi^2,$$

  where ρ_+^2 is defined by $\rho^2 \equiv r_+^2 + a^2\cos^2\theta$
- This is *not* the line interval of a 2-sphere.

Thus the Kerr horizon has constant Boyer–Lindquist coordinate $r = r_+$ but it is not spherical.

From the line element

$$d\sigma^2 = \rho_+^2 d\theta^2 + \left(\frac{2Mr_+}{\rho_+}\right)^2 \sin^2\theta\, d\varphi^2,$$

the metric tensor for the Kerr horizon is

$$g = \begin{pmatrix} \rho_+^2 & 0 \\ 0 & \left(\frac{2Mr_+}{\rho_+}\right)^2 \sin^2\theta \end{pmatrix}$$

The area of the Kerr horizon is then

$$\begin{aligned} A_{\rm K} &= \int_0^{2\pi} d\varphi \int_0^{\pi} \sqrt{\det g}\; d\theta \\ &= 2Mr_+ \int_0^{2\pi} d\varphi \int_0^{\pi} \sin\theta\, d\theta \\ &= 8\pi M r_+ = 8\pi M\left(M + \sqrt{M^2 - a^2}\right). \end{aligned}$$

The horizon area for a Schwarzschild black hole is obtained by setting $a = 0$ in this expression, corresponding to vanishing angular momentum, in which case $r_+ = 2M$ and

$$A_{\rm S} = 16\pi M^2 = 4\pi(2M)^2,$$

as expected for a spherical horizon of radius $2M$.

18.4.5 Orbits in the Kerr Metric

We may take a similar approach as in the Schwarzschild metric to determine the orbits of particles and photons.

- In the Kerr metric orbits are not confined to a plane (only axial, not full spherical symmetry).
- To simplify, we shall consider only motion in the equatorial plane ($\theta = \frac{\pi}{2}$) to illustrate concepts.

The Kerr line element with that restriction is then

$$ds^2 = -\left(1 - \frac{2M}{r}\right) dt^2 - \frac{4Ma}{r} d\varphi dt + \frac{r^2}{\Delta} dr^2 + \left(r^2 + a^2 + \frac{2Ma^2}{r}\right) d\varphi^2.$$

There are two conserved quantitities,

$$\varepsilon = -\xi_t \cdot u \qquad \ell = \xi_\varphi \cdot u,$$

At large distances from the gravitational source

- ε may be interpreted as the conserved energy per unit rest mass.
- ℓ may be interpreted as the angular momentum component per unit mass along the symmetry axis.

The corresponding Killing vectors are

$$\xi_t = (1,0,0,0) \qquad \xi_\varphi = (0,0,0,1).$$

and the norm of the 4-velocity provides the usual constraint

$$u \cdot u = -1.$$

From the Kerr metric

$$-\varepsilon = \xi_t \cdot u = g_{00}u^0 + g_{03}u^3 \qquad \ell = \xi_\varphi \cdot u = g_{30}u^0 + g_{33}u^3,$$

and solving for $u^0 = dt/d\tau$ and $u^3 = d\varphi/d\tau$ gives

$$\frac{dt}{d\tau} = \frac{1}{\Delta}\left[\left(r^2 + a^2 + \frac{2Ma^2}{r}\right)\varepsilon - \frac{2Ma}{r}\ell\right]$$

$$\frac{d\varphi}{d\tau} = \frac{1}{\Delta}\left[\left(1 - \frac{2M}{r}\right)\ell + \frac{2Ma}{r}\varepsilon\right].$$

By similar steps as for the Schwarzschild metric, this leads to the equations of motion

$$\frac{\varepsilon^2 - 1}{2} = \frac{1}{2}\left(\frac{dr}{d\tau}\right)^2 + V_{\text{eff}}(r, \varepsilon, \ell)$$

$$V_{\text{eff}}(r, \varepsilon, \ell) \equiv -\frac{M}{r} + \frac{\ell^2 - a^2(\varepsilon^2 - 1)}{2r^2} - \frac{M(\ell - a\varepsilon)^2}{r^3},$$

which are valid in the equatorial plane.

18.4.6 Frame Dragging

A striking feature of the Kerr solution is *frame dragging:* loosely, the black hole drags spacetime with it as it rotates.

- This arises ultimately because the Kerr metric contains off-diagonal components $g_{03} = g_{30}$.
- One consequence is that a particle dropped radially onto a Kerr black hole will acquire non-radial components of motion as it falls freely in the gravitational field.

Let's investigate by calculating $d\varphi/dr$ for a particle dropped from rest ($\varepsilon = 1$) with zero angular momentum ($\ell = 0$) onto a Kerr black hole (in the equatorial plane). Since $\varepsilon = 1$ and $\ell = 0$ are conserved on the geodesic, from earlier equations,

$$\frac{d\varphi}{d\tau} = \frac{1}{\Delta}\left[\left(1 - \frac{2M}{r}\right)\ell + \frac{2Ma}{r}\varepsilon\right] \quad \longrightarrow \quad \frac{d\varphi}{d\tau} = \frac{1}{\Delta}\left(\frac{2Ma}{r}\right),$$

$$\frac{\varepsilon^2 - 1}{2} = \frac{1}{2}\left(\frac{dr}{d\tau}\right)^2 + V_{\text{eff}}(r, \varepsilon, \ell) \quad \longrightarrow \quad \frac{dr}{d\tau} = \sqrt{\frac{2M}{r}\left(1 + \frac{a^2}{r^2}\right)},$$

which may be combined to give

$$\frac{d\varphi}{dr} = \frac{d\varphi/d\tau}{dr/d\tau} = -\frac{2Ma}{r\Delta}\left[\frac{2M}{r}\left(1 + \frac{a^2}{r^2}\right)\right]^{-1/2}.$$

The particle is dragged in angle φ as it falls radially inward, *even though no forces act on it.*

This effect is termed *"dragging of inertial frames"* and produces a gyroscopic precession termed the *Lense–Thirring effect.*

> NASA's Gravity Probe B used 4 gyroscopes aboard a satellite in an orbit almost directly over the poles to look for gyroscopic precession giving direct evidence of frame dragging by the rotating gravitational field of the Earth.

In the Kerr metric

$$p^{\varphi} \equiv p^3 = g^{3\mu} p_\mu = g^{33} p_3 + g^{30} p_0,$$

$$p^t \equiv p^0 = g^{0\mu} p_\mu = g^{00} p_0 + g^{03} p_3,$$

$$p^0 \equiv m\frac{dt}{d\tau} \qquad p^3 \equiv m\frac{d\varphi}{d\tau},$$

and combining these relations gives an expression for $d\varphi/dt$,

$$\frac{d\varphi}{dt} = \frac{d\varphi/d\tau}{dt/d\tau} = \frac{p^3}{p^0} = \frac{g^{33}p_3 + g^{30}p_0}{g^{00}p_0 + g^{03}p_3}.$$

If we consider a zero angular momentum particle (in the equatorial plane), then $p^3 = 0$ and

$$\omega(r,\theta) \equiv \frac{d\varphi}{dt} = \frac{g^{30}}{g^{00}} = \frac{g^{\varphi t}}{g^{tt}}.$$

> $\omega(r,\theta)$ is termed the *angular velocity of a zero angular momentum particle*; it measures the frame dragging.

The Kerr line element defines the covariant components of the Kerr metric $g_{\mu\nu}$. To evaluate

$$\omega(r,\theta) = \frac{g^{\varphi t}}{g^{tt}}$$

we need $g^{\mu\nu}$, which may be obtained as the matrix inverse of $g_{\mu\nu}$. The metric is diagonal in r and θ so

$$g^{rr} = g_{rr}^{-1} = \frac{\Delta}{\rho^2} \qquad g^{\theta\theta} = g_{\theta\theta}^{-1} = \frac{1}{\rho^2},$$

and we need only evaluate

$$g^{-1} = \begin{pmatrix} g_{tt} & g_{t\varphi} \\ g_{\varphi t} & g_{\varphi\varphi} \end{pmatrix}^{-1}$$

to obtain the other non-zero entries for $g^{\mu\nu}$. Letting

$$D = \det g = g_{tt}g_{\varphi\varphi} - (g_{t\varphi})^2,$$

the matrix inverse is

$$g^{-1} = \frac{1}{D}\begin{pmatrix} g_{\varphi\varphi} & -g_{t\varphi} \\ -g_{\varphi t} & g_{tt} \end{pmatrix}.$$

Inserting explicit expressions for the $g_{\mu\nu}$ and carrying out some algebra yields

$$\omega(r,\theta) = \frac{g^{\varphi t}}{g^{tt}} = \frac{2Mra}{(r^2+a^2)^2 - a^2\Delta\sin^2\theta}.$$

18.4.7 Innermost Stable Circular Orbit and Binding Energy

The property of particle orbits in the Kerr metric that is probably of most interest in astrophysics is the *binding energy of the innermost stable circular orbit,* since this is related to the energy that can be extracted from accretion on a rotating black hole.

If we denote the radius of the innermost stable orbit by R, for circular orbits we have that $dr/d\tau = 0$ and from earlier

$$\frac{\varepsilon^2 - 1}{2} = \frac{1}{2}\left(\frac{dr}{d\tau}\right)^2 + V_{\text{eff}}(r, \varepsilon, \ell) \quad \longrightarrow \quad \frac{\varepsilon^2 - 1}{2} = V_{\text{eff}}(R, \varepsilon, \ell).$$

Furthermore, to remain circular the radial acceleration must vanish,

$$\left.\frac{\partial V_{\text{eff}}}{\partial r}\right|_{r=R} = 0,$$

and to be a stable orbit the potential must be a minimum, which requires the second derivative to be positive,

$$\left.\frac{\partial^2 V_{\text{eff}}}{\partial r^2}\right|_{r=R} \geq 0,$$

with equality holding for the last stable orbit.

This set of equations may be solved to determine the innermost stable orbit and its binding energy.

For extremal black holes ($a = M$), one finds that

1. Co-rotating orbits (accretion orbits revolving in the same sense as the rotation of the hole) are more stable than the corresponding counter-rotating orbits.

2. For co-rotating orbits,

$$\varepsilon = \frac{1}{\sqrt{3}} \qquad \ell = \frac{2M}{\sqrt{3}} \qquad R = M.$$

3. The quantity ε is the energy per unit rest mass measured at infinity, so the binding energy per unit rest mass, B/M, is given by

$$\frac{B}{M} = 1 - \varepsilon.$$

4. These equations imply that the fraction f of the rest mass that could theoretically be extracted is

$$f = 1 - \varepsilon = 1 - \frac{1}{\sqrt{3}} \simeq 0.42.$$

for a transition from a distant unbound orbit to the innermost circular bound orbit of a Kerr black hole.

Therefore, in principle 42% of the rest mass of accreted material could be extracted as usable energy by accretion onto an extreme Kerr black hole.

- One expects less efficiency than this for actual situations, but optimistically one might expect as much as *20–30% efficiencies* in realistic accretion scenarios.
- Compare with the maximum theoretical efficiency of *6% for accretion on a spherical black hole.*
- Compare with the *0.7% efficiency for hydrogen fusion* in the conversion of rest mass to usable energy.

Accretion onto rotating black holes is a *very efficient mechanism* for converting mass to energy.

18.4.8 The Ergosphere

- With capable propulsion, an observer could remain stationary at any point outside the event horizon of a Schwarzschild black hole.
- No amount of propulsion can enable an observer to remain stationary inside a Schwarzschild horizon (causality violation).
- We now demonstrate that, for a rotating black hole, even outside the horizon it may be impossible for an observer to remain stationary.

For a stationary observer

$$u^{\mu}_{\text{obs}} = (u^0_{\text{obs}}, 0, 0, 0) = \left(\frac{dt}{d\tau}, 0, 0, 0\right).$$

Writing out the condition $u_{\text{obs}} \cdot u_{\text{obs}} = -1$ for the Kerr metric gives

$$u_{\text{obs}} \cdot u_{\text{obs}} = g_{00}(u^0_{\text{obs}})^2 = -1$$

But

$$g_{00} = -\left(1 - \frac{2Mr}{\rho^2}\right) = -\left(1 - \frac{2Mr}{r^2 + a^2\cos^2\theta}\right) = -\left(\frac{r^2 + a^2\cos^2\theta - 2Mr}{r^2 + a^2\cos^2\theta}\right)$$

vanishes if

$$r^2 - 2Mr + a^2\cos^2\theta = 0$$

Generally then, solving the above quadratic for r

- $g_{00} = 0$ on the surface defined by

$$r_{\text{e}}(\theta) = M + \sqrt{M^2 - a^2\cos^2\theta},$$

- $g_{00} > 0$ inside this surface.
- $g_{00} < 0$ outside this surface.

Therefore, since $(u^0_{\text{obs}})^2$ *must be positive,* the condition

$$u_{\text{obs}} \cdot u_{\text{obs}} = g_{00}\underbrace{(u^0_{\text{obs}})^2}_{+} = -1$$

cannot be satisfied for any observer having $r \leq r_{\text{e}}(\theta)$ (since then $g_{00} > 0$).

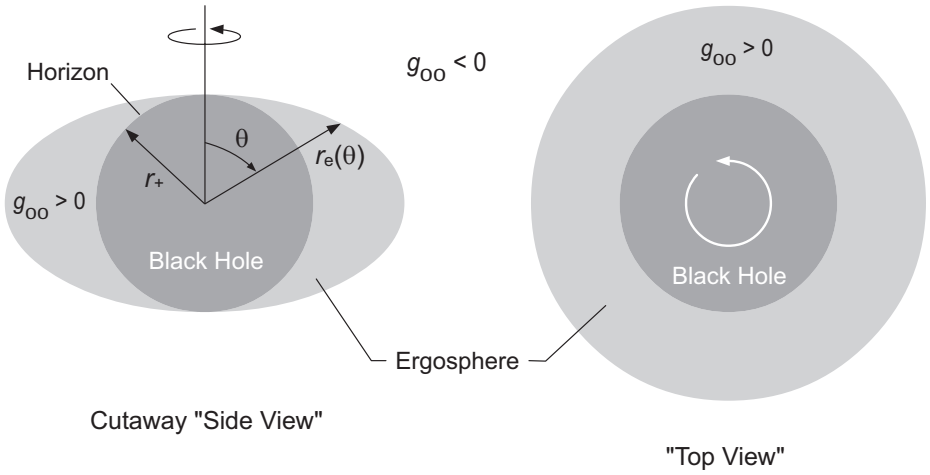

Figure 18.20: The ergosphere of a Kerr black hole. Note that the horizon lies at a constant value of r but it is not a spherical surface.

Comparing

$$r_+ = M + \sqrt{M^2 - a^2} \qquad r_e(\theta) = M + \sqrt{M^2 - a^2\cos^2\theta},$$

we see that

- If $a \neq 0$ the surface $r_e(\theta)$ generally lies outside the horizon r_+, except at the poles, where the two surfaces are coincident (Figure 18.20).
- If $a = 0$, the Kerr black hole reduces to a Schwarzschild black hole, in which case r_+ and $r_e(\theta)$ define the same surface.

The region lying between $r_e(\theta)$ and the horizon r_+ is termed the *ergosphere*.

From preceding considerations, there can be *no stationary observers within the ergosphere.* Further insight comes from considering the motion of photons within the ergosphere.

- Assume photons within the ergosphere moving tangent to a circle at constant r in the equatorial plane $\theta = \frac{\pi}{2}$, so $dr = d\theta = 0$.
- Since they are photons, $ds^2 = 0$ and from the Kerr line element with $dr = d\theta = 0$,

$$ds^2 = 0 \quad \rightarrow \quad g_{00}\,dt^2 + 2g_{03}\,dt\,d\varphi + g_{33}\,d\varphi^2 = 0.$$

- Divide both sides by dt^2 to give a quadratic equation in $d\varphi/dt$

$$g_{00} + 2g_{03}\frac{d\varphi}{dt} + g_{33}\left(\frac{d\varphi}{dt}\right)^2 = 0$$

Thus, solving the quadratic for $d\varphi/dt$

$$\begin{aligned}\frac{d\varphi}{dt} &= \frac{-2g_{03} \pm \sqrt{4g_{03}^2 - 4g_{33}g_{00}}}{2g_{33}} \\ &= -\frac{g_{03}}{g_{33}} \pm \sqrt{\left(\frac{g_{03}}{g_{33}}\right)^2 - \frac{g_{00}}{g_{33}}},\end{aligned}$$

where

- $+$ is associated with motion opposite black hole rotation.
- $-$ is associated with motion with black hole rotation.

- Now g_{00}
  - *vanishes at the boundary* of the ergosphere and
  - is *positive inside the boundary.*
- Setting $g_{00} = 0$ in

$$\frac{d\varphi}{dt} = -\frac{g_{03}}{g_{33}} \pm \sqrt{\left(\frac{g_{03}}{g_{33}}\right)^2 - \frac{g_{00}}{g_{33}}},$$

  gives two solutions,

$$\underbrace{\frac{d\varphi}{dt} = 0}_{\text{opposite rotation}} \qquad \underbrace{\frac{d\varphi}{dt} = -\frac{2g_{03}}{g_{33}}}_{\text{with rotation}},$$

> The photon sent backwards against the hole rotation at the surface of the ergosphere is stationary in φ!

- Obviously a particle, which must have a velocity less than a photon, must rotate with the black hole irrespective of the amount of angular momentum that it has.
- Inside the ergosphere $g_{00} > 0$, so all photons and particles must *rotate with the hole.*

> In essence, the frame dragging for $r < r_e(\theta)$ is so severe that *speeds in excess of light* would be required for an observer to remain at rest with respect to infinity.

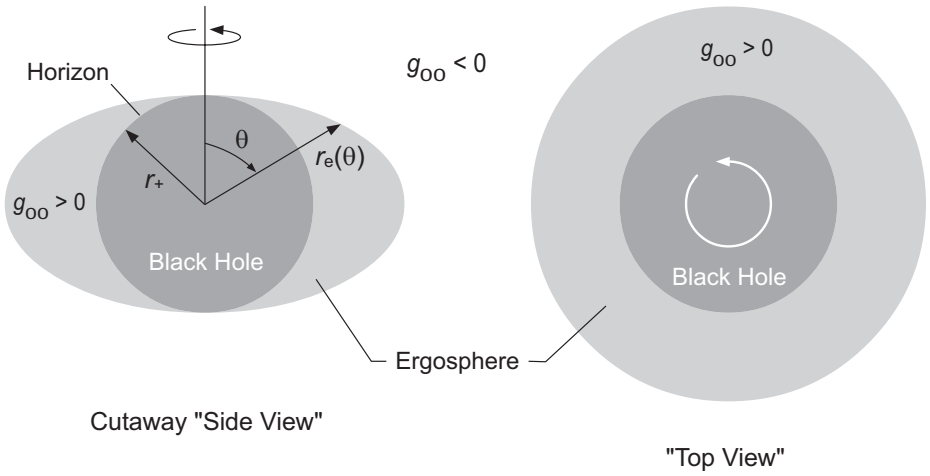

- In the limit $a = J/M \to 0$, where the angular momentum of the Kerr black hole vanishes,

$$r_e(\theta) = M + \sqrt{M^2 - a^2 \cos^2\theta} \quad \to \quad 2M$$

  and becomes *coincident with the Schwarzschild horizon.*

- Thus, rotation
  - has extended the region $r < 2M$ of the spherical black hole where no stationary observers can exist to
  - a larger region $r < r_e(\theta)$ surrounding the rotating black hole where *no observer can remain at rest because of frame dragging effects.*

- This ergospheric region
  - lies *outside* the horizon, implying that
  - a particle could enter it and *still escape* from the black hole.

18.4.9 Extraction of Rotational Energy from Black Holes

We have seen that quantum vacuum fluctuations allow mass to be extracted from a Schwarzschild black hole as Hawking radiation, but it is impossible to extract mass from a *classical* Schwarzschild black hole (it all lies within the event horizon).

- However, the existence of separate surfaces defining the ergosphere and the horizon for a Kerr black hole implies the possibility of extracting rotational energy from a *classical* black hole.
- The simplest way to demonstrate the feasibility of extracting rotational energy from a black hole is through a *Penrose process*.

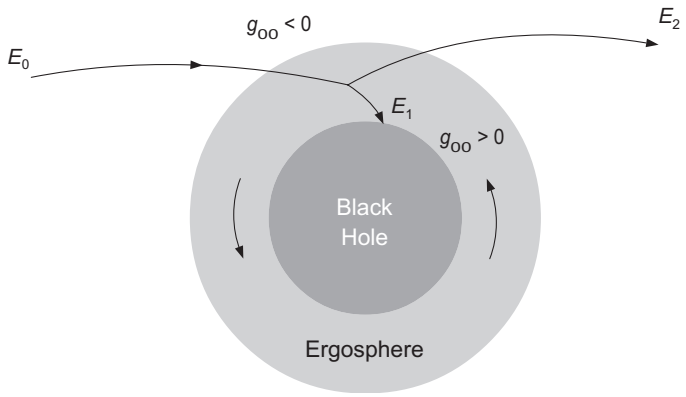

Figure 18.21: A Penrose process.

A Penrose process is illustrated schematically in Fig. 18.21.

- A particle falls into the ergosphere of a Kerr black hole and decays into two particles. One falls through the horizon; one exits the ergosphere and escapes to infinity.
- The decay within the ergosphere is a local process. By equivalence principle arguments, it may be analyzed in a freely falling frame according to the usual rules of scattering theory.
- In the decay 4-momentum p is conserved

$$p_0 = p_2 + p_1$$

(NOTE: subscripts label particles, not components!)

- $p = (-E, \boldsymbol{p})$ and $\xi_t = (1,0,0,0)$, so $E = -p\cdot\xi_t$. Thus, if the particle 2 scattering to infinity has rest mass m_2, its energy is

$$E_2 = -p_2\cdot\xi_t = -\frac{m_2}{m_2}\,p_2\cdot\xi_t = -m_2\,\underbrace{p_2\frac{\xi_t}{m_2}}_{-\varepsilon} = m_2\varepsilon$$

where $\varepsilon = -\xi_t\cdot u = -\xi_t\cdot(p/m)$ has been used.

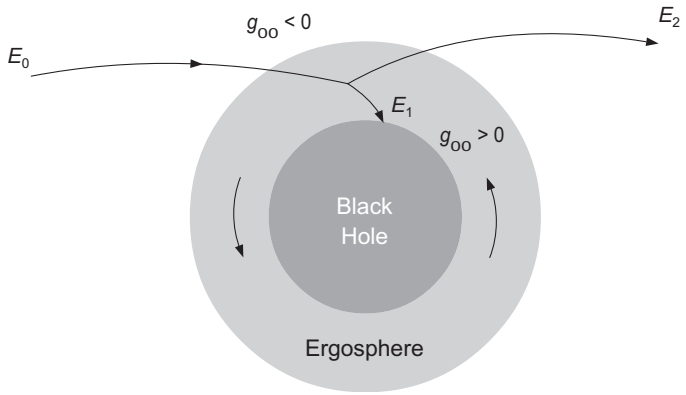

- Taking the scalar product of $p_0 = p_2 + p_1$ with ξ_t

$$p_0 \cdot \xi_t = (p_2 + p_1) \cdot \xi_t$$

yields the requirement,

$$E_2 = E_0 - E_1.$$

since $E = -\xi_t \cdot p$.

- If particle 1 were to reach ∞ instead of crossing the event horizon of the black hole, E_1 would necessarily be positive so

1. $E_2 < E_0$
2. Less energy would be emitted than put in.

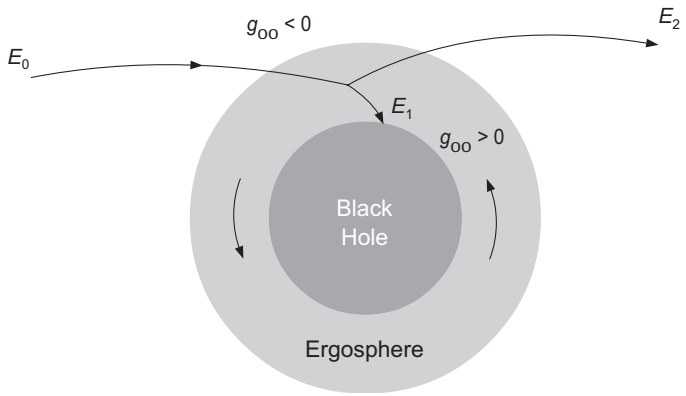

However . . .

- For the Killing vector $\xi_t = (1,0,0,0)$,

$$\begin{aligned}\xi_t \cdot \xi_t &= g_{\mu\nu}\xi_t^{\mu}\xi_t^{\nu} \\ &= g_{00}\xi_t^0\xi_t^0 = g_{00} = -\left(1 - \frac{2Mr}{\rho^2}\right),\end{aligned}$$

  and g_{00} vanishes on the surface $r_e(\theta)$ and is positive inside it.

- Therefore, *within the ergosphere* ξ_t *is a spacelike vector:*

$$\xi_t \cdot \xi_t = g_{00} > 0 \qquad \text{(within the ergosphere)}.$$

- By arguments similar to those concerning Hawking radiation,

  1. $-E_1$ is not an energy within the ergosphere but is a component of spatial momentum, which can have either a *positive or negative value (!)*.
  2. For those decays where the trajectories are arranged such that $E_1 < 0$, we obtain from $E_2 = E_0 - E_1$ that $E_2 > E_0$ and *net energy is extracted* in the Penrose process.

The energy extracted in the Penrose process comes at the expense of the rotational energy of the Kerr black hole.

- For trajectories with $E_1 < 0$, the captured particle adds a negative angular momentum, thus reducing the angular momentum and total energy of the black hole to just balance the angular momentum and total energy carried away by the escaping particle.
- A series of Penrose events could extract all the angular momentum of a Kerr black hole, leaving a Schwarzschild black hole.
- No further energy can then be extracted from the resulting spherical black hole (except by quantum Hawking processes).

The Penrose mechanism establishes *proof of principle* in a simple model that the rotational energy of Kerr black holes is externally accessible in classical processes.

- Practically, Penrose processes are not likely to be important in astrophysics because the required conditions are not easily realized.
- Instead, the primary sources of emitted energy from black hole systems likely come from
  1. Complex electromagnetic coupling of rotating black holes to external accretion disks and jets.
  2. Gravitational energy released by accretion onto black holes.

There is very strong observational evidence for such processes in a variety of astrophysical environments.

18.5 Black Hole Theorems and Conjectures

In this section we summarize (in a non-rigorous way) a set of theorems and conjectures concerning black holes. Some we have already used in various contexts.

- Singularity theorems: Loosely, any gravitational collapse that proceeds far enough results in a spacetime singularity.
- Cosmic censorship conjecture: All spacetime singularities are hidden by event horizons (*no naked singularities*).
- (Classical) area increase theorem: In all classical processes involving horizons, the area of the horizons can never decrease.
- Second law of black hole thermodynamics: Where quantum mechanics is important the classical area increase theorem is replaced by

    1. The entropy of a black hole is proportional to the surface area of its horizon.
    2. The total entropy of the Universe can never decrease an any process.

- The no-hair theorem/conjecture: If gravitational collapse to a black hole is nearly spherical,
  - All non-spherical parts of the mass distribution (quadrupole moments, . . .) except angular momentum are radiated away as gravitational waves.
  - Horizons eventually become stationary.
  - A stationary black hole is characterized by three numbers: the mass M, the angular momentum J, and the charge Q.
  - M, J, and Q are all determined by fields *outside* the horizon, not by integrals over the interior.

The most general solution characterized by M, J, and Q is termed a *Kerr–Newman black hole.* However,

- It is likely that the astrophysical processes that could form a black hole would neutralize any excess charge.
- Thus astrophysical black holes are Kerr black holes (the Schwarzschild solution being a special case of the Kerr solution for vanishing angular momentum).

The "No Hair Theorem": black holes destroy all details (*the hair*) about the matter that formed them, leaving behind only M, J, and possibly Q as observable external characteristics.

- Birkhoff's theorem: The Schwarzschild solution is the *only* spherically symmetric solution of the vacuum Einstein equations. (The static assumption is, in fact, a consequence of the spherical symmetry assumption.)

These theorems and conjectures place the mathematics of black holes on reasonably firm ground. To place the *physics* of black holes on firm grounds, these ideas must be tested by observation, to which we now turn.

18.6 Observation of Stellar Black Holes

We have very strong reasons to believe that black holes exist and are being observed indirectly because of

1. Unseen massive companions in binary star systems that are
   - Strong sources of X-rays
   - Probably too massive to be anything other than black holes.
2. The centers of many galaxies where
   - Masses inferred by virial theorem methods (or even direct measurement of individual star orbits in the center of the Milky Way) are far too large to be accounted for by any simple hypothesis other than a supermassive black hole.
   - In many cases there is direct evidence of an enormous energy source in the center of the galaxy.

   We first summarize some of the reasons why the first class of observations give us strong confidence that black holes, or at least objects that have many of the features of black holes, exist.

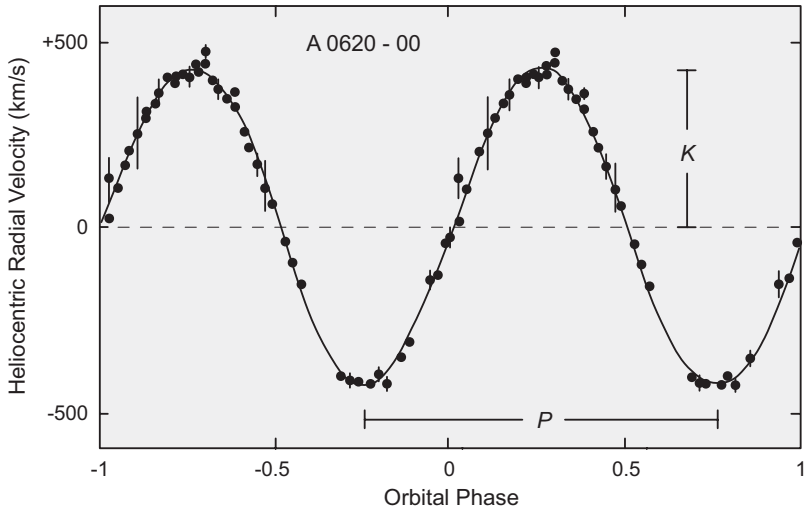

Figure 18.22: Velocity curve for the black hole binary candidate A 0620–00.

18.6.1 Black Hole Masses in X-ray Binaries

From Kepler's laws, the mass function $f(M)$ for the binary may be related to the radial velocity curve (Fig. 18.22) through

$$f(M) = \frac{(M \sin i)^3}{(M + M_c)^2} = \frac{PK^3}{2\pi G}$$
$$= 0.1036 \left(\frac{P}{1\ \text{day}}\right) \left(\frac{K}{100\ \text{km s}^{-1}}\right)^3 M_\odot$$

where

- K is the semiamplitude and P the period of the radial velocity.
- i is the tilt angle of the orbit
- M_c is the mass of the companion star.
- M is the mass of the black hole

Table 18.1: Some black hole candidates in galactic X-ray binaries

X-ray source	Period (days)	$f(M)$	$M_c(M_\odot)$	$M(M_\odot)$
Cygnus X-1	5.6	0.24	24–42	11–21
V404 Cygni	6.5	6.26	$\sim$0.6	10–15
GS 2000+25	0.35	4.97	$\sim$0.7	6–14
H 1705–250	0.52	4.86	0.3–0.6	6.4–6.9
GRO J1655–40	2.4	3.24	2.34	7.02
A 0620–00	0.32	3.18	0.2–0.7	5–10
GS 1124–T68	0.43	3.10	0.5–0.8	4.2–6.5
GRO J0422+32	0.21	1.21	$\sim$0.3	6–14
4U 1543–47	1.12	0.22	$\sim$2.5	2.7–7.5

Because the angle *i* is often not known,

- The measured mass function places a lower limit on the mass of the unseen component of the binary if the mass of the companion star is known.
- The mass of the companion can often be estimated reliably from systematic spectral features.

Table 18.1 illustrates some candidate binary star systems where a mass function analysis suggests an unseen companion too massive to be a white dwarf or neutron star. We assume these to be black holes.

18.6.2 Example: Cygnus X-1

The first strong case found, and most famous stellar black hole candidate, is Cygnus X-1 .

1. In the early 1970s an X-ray source was discovered in Cygnus and designated Cygnus X-1.
2. In 1972, a radio source was found in the same general area and identified optically with a blue supergiant star called HDE226868.
3. Correlations in radio activity of HDE226868 and X-ray activity of Cygnus X-1 implied that the two were probably components of the same binary system.
4. Doppler measurements of the radial velocity of HDE226868 and other data confirmed that it was a member of a binary with a period of 5.6 days.
5. Detailed analysis showed that the X-ray source was fluctuating in intensity on timescales as short as 1/1000 of a second.

    - Signals controlling the fluctuation are limited by light speed, which implies that the X-ray source must be very compact, probably no more than hundreds of kilometers in diameter.
    - The
        - small size,
        - orbital perturbation on HDE226868, and
        - strong X-ray emission,

      indicate that Cygnus X-1 is a compact object (white dwarf, neutron star, or black hole, with the latter two possibilities more likely).

5. The mass of the blue supergiant HDE226868 was estimated from known properties of such stars (it is a spectrum and luminosity class O9.7Iab star).

   - This, coupled with a mass function analysis, can be used to estimate the mass of the unseen, compact companion.
   - These estimates are uncertain because the geometry (tilt of the binary orbit) can only partially be inferred from data.
   - However, all such estimates place a lower limit of about 5–6 $M_\odot$ on the unseen companion and more likely indicate a mass near 10 $M_\odot$.

6. Since we know of no conditions that would permit a neutron star to exist above about 2–3 solar masses (or a white dwarf above about 1.4 solar masses), we conclude that the unseen companion must be a black hole.

Although this chain of reasoning is indirect, it builds a very strong case that Cygnus X-1 contains a black hole.

18.7 Supermassive Black Holes in the Cores of Galaxies

Many observations of star motion near the centers of galaxies indicate the presence of large, unseen mass concentrations. The most direct is for our own galaxy.

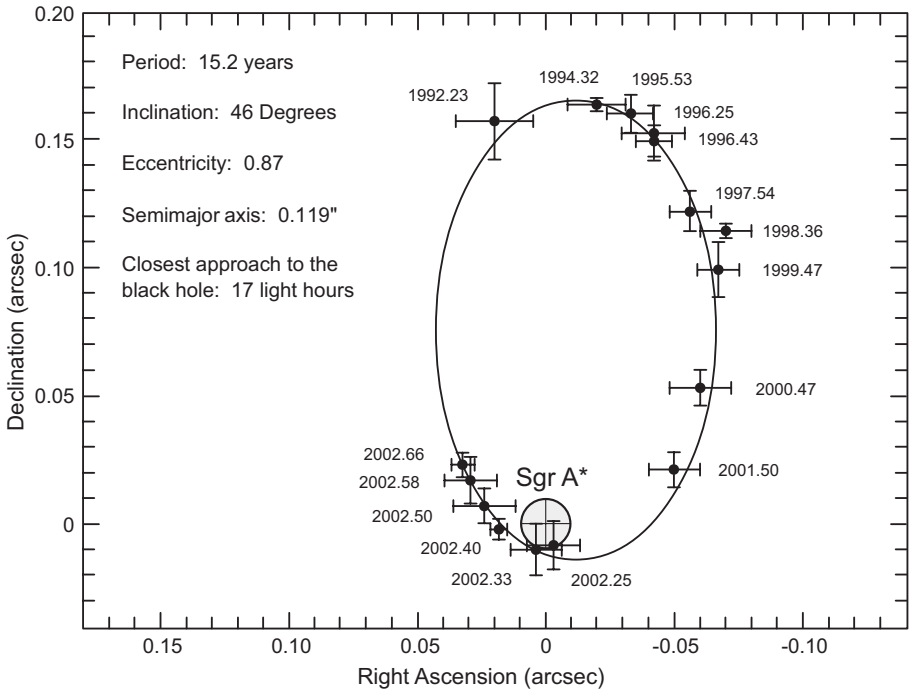

Figure 18.23: Orbit of the star S2 near the radio source SGR A*.

18.7.1 The Black Hole at the Center of the Milky Way

The star denoted S2 is a 15 solar mass main sequence star that orbits in the vicinity of the strong radio source SGR A*, which is thought to lie very near the center of the Milky Way.

- The orbit has been measured precisely using adaptive optics and speckle interferometry at near-IR wavelengths (penetrate dust).
- The orbit of S2 is shown in Fig. 18.23, with dates shown in fractions of a year beginning in 1992.
- The orbit corresponds to the projection of the best-fit ellipse with SGR A* at a focus. The closest approach for the orbit corresponds to a distance of about 17 light hours from SGR A*.

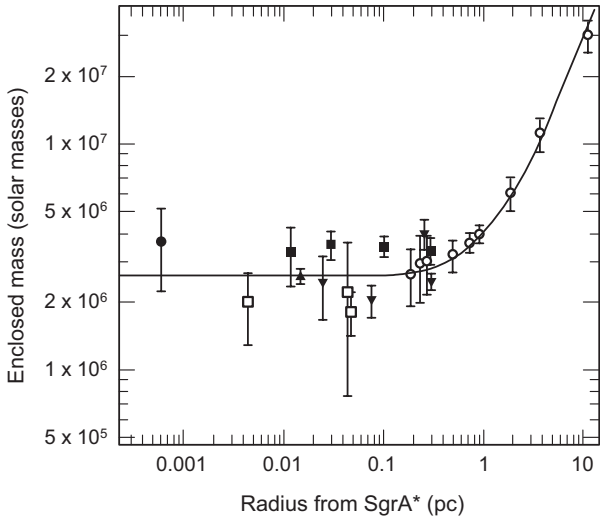

Figure 18.24: Mass distribution near Sag A* as inferred from stellar motion.

- From detailed fits to the Kepler orbit of S2, the mass inside the orbit of the star is estimated to be $2.6 \times 10^6 M_\odot$ (see Fig. 18.24).
- From the size of the orbit, this mass is concentrated in a region that cannot be much larger than the Solar System, with little luminous mass in that region.
- By far the simplest explanation is that the radio source SGR A* coincides with a nearly 3 million solar mass black hole.
- The innermost point in Fig. 18.24 is derived from the observed elliptical orbit for the star S2 that comes within 17 light hours of the black hole
  - This distance is still well outside the tidal distortion radius for the star (which is about 16 light minutes).
  - It is about 2100 times larger than the event horizon.
  - At closest approach the separation from the black hole is not much larger than the radius of the Solar System.

18.7.2 The Water Masers of NGC 4258

The galaxy NGC 4258 (also called M106) is an Sb spiral visible through a small telescope, but its nucleus is moderately active and it is also classified as a Seyfert 2 Active Galactic Nucleus (AGN). It lies in the constellation Canes Venatici (very near the Big Dipper) at a distance of around 20 Mpc. This makes it one of the nearest AGNs.

- A set of masers has been observed in the central region of the galaxy. (Masers are the microwave analog of a visible-light laser.) The maser emission in NGC 4258 is due to clouds of heated water vapor, so these are termed water masers.
- Because masers produce sharp spectral lines (allowing precise Doppler shifts), and because microwaves are not strongly attenuated by the gas and dust near the nucleus of the galaxy, observation of the water masers has permitted the motion of gas near the center to be mapped very precisely using the Very Long Baseline Array (VLBA).

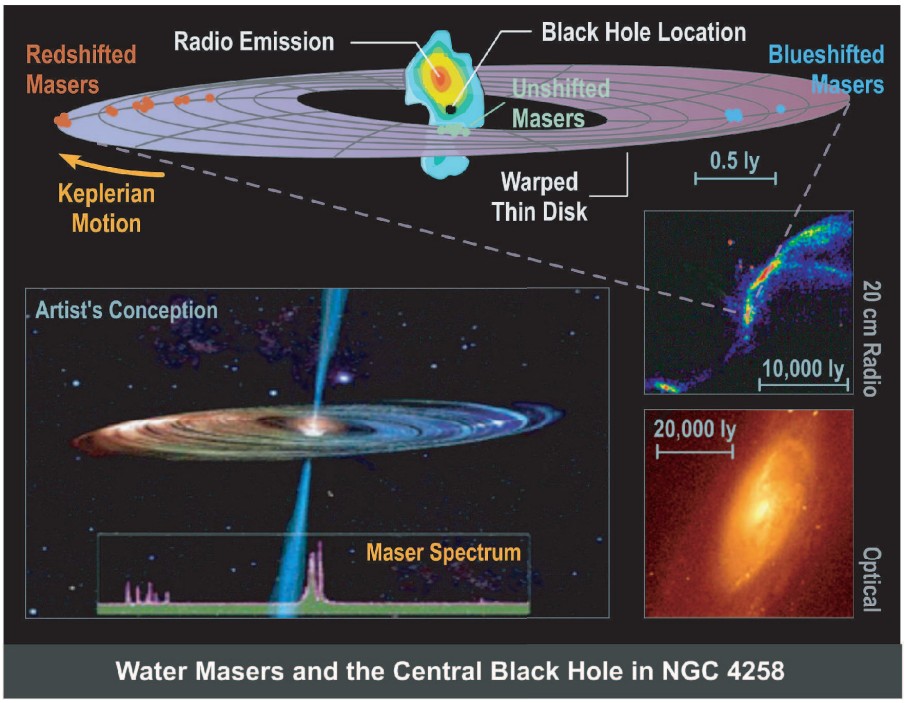

Figure 18.25: Water masers in NGC 4258 and evidence for a central black hole.

Water maser emission from the central region of NGC 4258 implies (Fig. 18.25).

- The masers are mapped with a precision of better than 1 milliarcsecond and their radial velocities indicate bulk motion of the gas within several light years of the core at velocities approaching 1000 km s^{-1}.
- In Fig. 18.25 masers approaching us (blue shift) are shown in blue, masers receding from us (red shift) are shown in red, and those with no net radial velocity are shown in green. From this we may infer the general rotation of the gas disk, as indicated by the arrow labeled “Keplerian motion”.

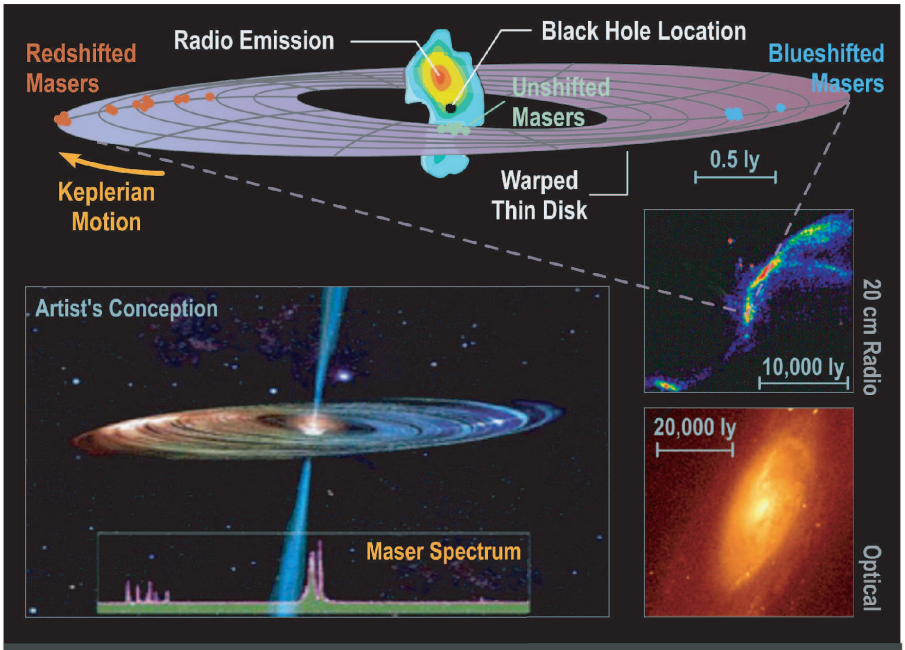

Water Masers and the Central Black Hole in NGC 4258

- The masers are embedded in a thin, warped, dusty, molecular gas disk revolving around the core.
- The motion of the masers is Keplerian → masers in orbit around a large mass that is completely contained within all their orbits.
- The mass obtained is approximately $3.5 \times 10^6 M_\odot$.
- Measured mass and measured size of region enclosed by maser orbits implies a minimum density of $10^8 M_\odot$ per cubic light year.
  - 10,000 times more dense than any known star cluster.
  - If such a star cluster existed, calculations indicate that collisions of the stars would cause the stars of the cluster to drift apart or mutually collapse to a huge black hole.
  - Only plausible explanation is a supermassive black hole.

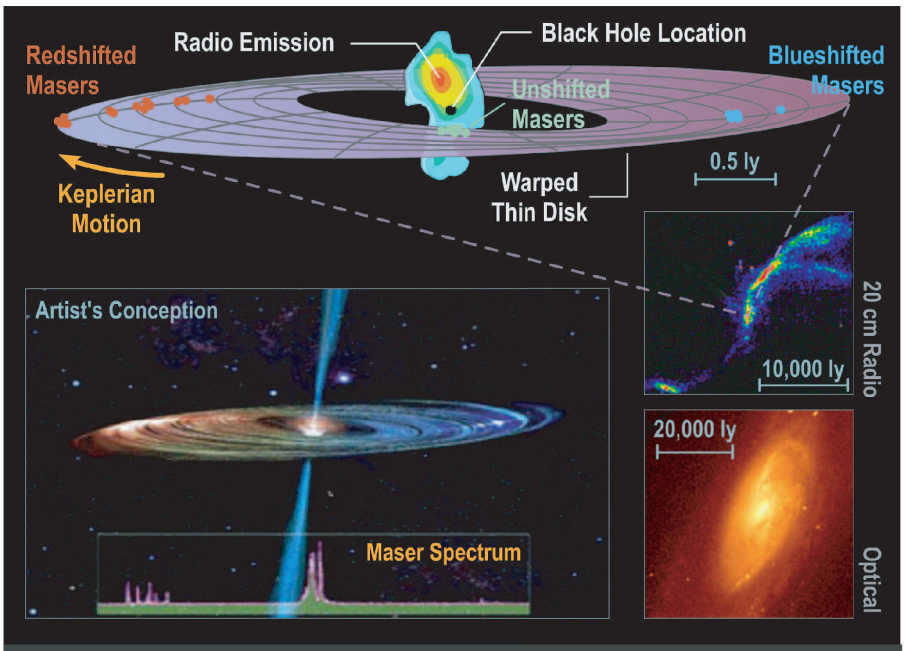

Water Masers and the Central Black Hole in NGC 4258

- The nucleus of the galaxy produces radio jets that appear to come from the dynamical center of the rotating disk and are approximately perpendicular to it (see fig).
- The position of the radio jets and precise location of the center of the disk determines the location of the central black hole engine within the uncertainty of the black circle shown in the figure.
  - This black circle denotes the uncertainty in location of the black hole, not its size.
  - The black circle is about 0.05 ly in diameter, but the supermassive black hole would have an event horizon hundreds of times smaller than this.

These results taken together make NGC 4258 one of the strongest cases known for the presence of supermassive black hole engines at the cores of active galactic nuclei.

18.7.3 Virial Methods and Central Masses

For distant galaxies we have insufficient telescopic resolution to track individual stars but we may still learn something about the mass contained within particular regions by observing the average velocities of stars in that region.

- On conceptual grounds, we may expect that the larger the gravitational field that stars feel, the faster they will move.
- This intuitive idea may be quantified by using the virial theorem to show that the mass M responsible for the gravitational field in which stars move in some spherical region of radius R is given by

$$M \simeq \frac{5R\sigma_{\rm r}^2}{G},$$

where the radial velocity dispersion

$$\sigma_{\rm r}^2 = \langle v_{\rm r}^2 \rangle \equiv \frac{1}{3N}\sum_{i=1}^{N} v_i^2$$

can be determined by averaging over the squares of radial velocity fields determined from Doppler-shift measurements.

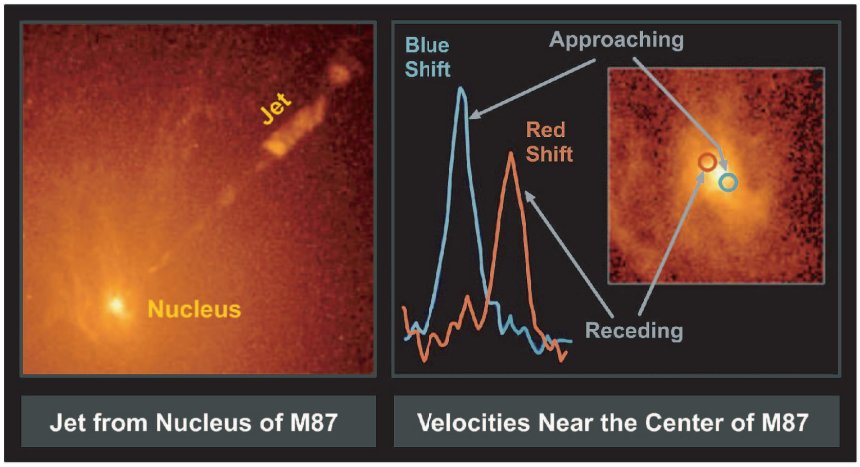

Figure 18.26: Evidence for a central black hole in the galaxy M87.

18.7.4 Evidence for a Supermassive Black Hole in M87

The left portion of Fig. 18.26 is a Hubble Space Telescope image showing the center of the giant elliptical radio galaxy M87.

- The diagonal line emanating from the nucleus in the left image is a jet of high-speed electrons—a synchrotron jet—approximately 6500 light years (2 kpc) long.
- This is what would be expected for matter swirling around the supermassive black hole, with part of it falling forever into the black hole and part of it being ejected in a high-speed jet.
- The right side of Fig. 18.26 illustrates Doppler shift measurements made on the central region of M87 that suggest rapid motion of the matter near the center.

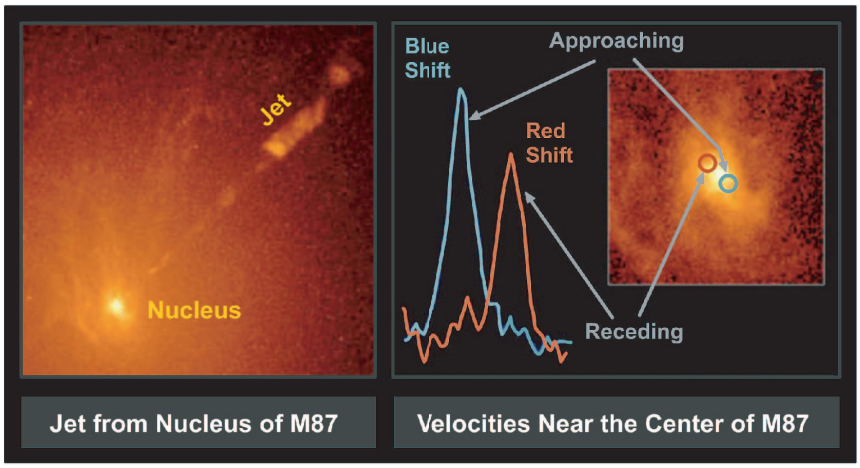

- The measurement was made by studying how the light from the disk is redshifted and blueshifted by the Doppler effect.
- The gas on one side of the disk is moving away from Earth at a speed of about 550 kilometers per second (redshift). The gas on the other side of the disk is approaching the Earth at the same speed (blueshift).
- These high velocities suggest a gravitational field produced by a huge mass concentration at the center of M87.
- By applying the virial theorem to the measured radial velocities we infer that approximately 3 billion solar masses are concentrated in a region at the galactic core that is only about the size of the Solar System.
- This inferred mass is far larger than could be accounted for by the visible matter there and the simplest interpretation is that a 3 billion solar mass black hole lurks in the core of M87.

18.8 Summary: A Strong But Circumstantial Case

The evidence cited in this chapter is not yet iron-clad proof of the existence of black holes.

- The defining characteristic of a black hole is an event horizon.
- No known black hole candidates are near enough to permit imaging an angular region the size of an event horizon with present instrumentation.
- (However, angular resolution sufficient to resolve the event horizon of the Milky Way's suspected central black hole appears at least technically feasible on a 2-decade timescale.)

Nevertheless, data on X-ray binary systems and on the motions of stars and other objects in the central region of our galaxy and other nearby ones provide extremely strong circumstantial evidence for the existence of black holes (or at least of objects very much like black holes).